Journal Pre-proofs

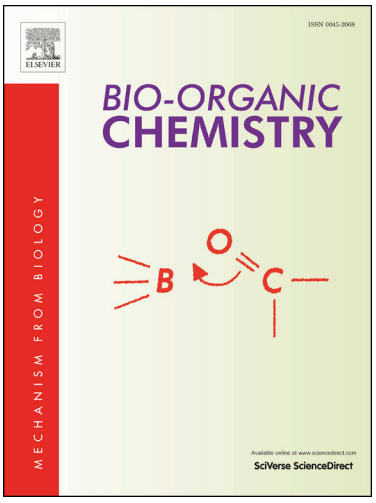

Exploration of Certain 1,3-Oxazole- and 1,3-Thiazole-Based Hydroxamic Acids as Histone Deacetylase Inhibitors and Antitumor Agents

Duong Tien Anh, Pham-The Hai, Le-Thi-Thu Huong, Eun Jae Park, Hye Won Jun, Jong Soon Kang, Joo-Hee Kwon, Do Thi Mai Dung, Vu Tran Anh, Van Thi My Hue, Sang-Bae Han, Nguyen-Hai Nam

PII: S0045-2068(20)31285-2
DOI: https://doi.org/10.1016/j.bioorg.2020.103988
Reference: YBIOO 103988

To appear in: *Bioorganic Chemistry*

Received Date: 8 March 2020
Revised Date: 14 April 2020
Accepted Date: 29 May 2020

Please cite this article as: D. Tien Anh, P-T. Hai, L-T. Huong, E. Jae Park, H. Won Jun, J. Soon Kang, J-H. Kwon, D. Thi Mai Dung, V. Tran Anh, V. Thi My Hue, S-B. Han, N-H. Nam, Exploration of Certain 1,3-Oxazole- and 1,3-Thiazole-Based Hydroxamic Acids as Histone Deacetylase Inhibitors and Antitumor Agents, *Bioorganic Chemistry* (2020), doi: https://doi.org/10.1016/j.bioorg.2020.103988

Exploration of Certain 1,3-Oxazole- and 1,3-Thiazole-Based Hydroxamic Acids as Histone Deacetylase Inhibitors and Antitumor Agents

Duong Tien Anh,[a] Pham-The Hai,[a] Le-Thi-Thu Huong,[a] Eun Jae Park, [b]Hye Won Jun,[b] Jong Soon Kang,[c] Joo-Hee Kwon,[c] Do Thi Mai Dung,[a] Vu Tran Anh,[a] Van Thi My Hue,[*,a] Sang-Bae Han,[*,b] Nguyen-Hai Nam,[*,a]

[a]*Hanoi University of Pharmacy, 13-15 Le Thanh Tong, Hanoi, Vietnam*
[b]*College of Pharmacy, Chungbuk National University, 194-31, Osongsaengmyung-1, Heungdeok, Cheongju, Chungbuk, 28160, Republic of Korea*
[c]*Laboratory Animal Resource Center, Korea Research Institute of Bioscience and Biotechnology, Cheongju, Chungbuk, Republic of Korea*

Abstract

Several novel series of hydroxamic acids bearing 2-benzamidooxazole/thiazole (**5a-g**, **6a-g**) or 2-phenylsulfonamidothiazole (**8a-c)** were designed and synthesized. The compounds were obtained straightforwards via a two step pathway, starting from commercially available ethyl 2-aminooxazole-4-carboxylate or ethyl 2-aminothiazole-4-carboxylate. Biological evaluation showed that these hydroxamic acids generally exhibited good cytotoxicity against three human cancer cell lines (SW620, colon; PC-3, prostate; NCI-H23, lung cancer), with IC_{50} values in low micromolar range and comparable to that of SAHA. These compounds also comparably inhibited HDACs with IC_{50} values in sub-micromolar range (0.010-0.131 μM) and some compounds (e.g **5f**, IC_{50}, 0.010 μM) were even more potent than SAHA (IC_{50}, 0.025 μM) in HDAC inhibition. Representative compounds **6a** and **8a** appeared to arrest the SW620 cell cycle at G2 phase and significantly induced both early and late apoptosis of SW620 colon cancer cells. Docking experiments on HDAC2 and HDAC6 isozymes revealed favorable interactions at the tunnel of the HDAC active site which positively contributed to the inhibitory activity of synthesized compound. The binding affinity predicted by docking program showed good correlation with the experimental IC_{50} values. This study demonstrates that simple 1,3-oxazole- and 1,3-thiazole-based hydroxamic acids are also promising as antitumor agents and HDAC inhibitors and these results should provide valuable information for further design of more potent HDAC inhibitors and antitumor agents.

Keywords: Histone deacetylase (HDAC) inhibitors, hydroxamic acids, docking, 1,3-oxazole, 1,3-thiazole.

***Corresponding authors:** Tel.: +84-4-39330531; Fax: +84-4-39332332; Emails: namnh@hup.edu.vn (N.H. Nam; V.T.M. Hue); shan@chungbuk.ac.kr (S.B. Han).

1. Introduction

Acetylation and deacetylation of the acetyl groups on the lysine amino tails of histone proteins are two opposite processes controlling the epigenetic balance [1]. Acetylation is catalyzed by histone acetyltransferases (HATs), while histone deacetylases (HDACs) are responsible for the catalytic removal of the acetyl groups on the histone lysine amino tails.[1] In mammalials, eighteen isoforms of HDACs have been described. These isoforms are divided into four classes (I-IV).[2, 3] It has been well documented that isoforms in class I (HDACs 1-3, 8) and class II (HDACs 4-6, 7, 9, 10) actively promote cell proliferation and block apoptosis, while preventing cellular differentiation, thus causing the cells growing continuously [2, 3]. HDAC isoforms 4, 6, 7 and 10 of class II have also been demonstrated to promote angiogenesis and cellular migration, two processes important for tumor metastatis [2, 3]. Due to their clear implication in the initiation and development of verious maligancies, HDACs have become a validated target for current anticancer drug design and development.[1-3] As a result, a number of structurally diverse HDAC inhibitors have been identified through intensive efforts of medicinal chemists worldwide. These include hydroxamic acids (e.g. SAHA or suberoylanilide hydroxamic acid), cyclic peptide (e.g. depsipeptide), short-chain fatty acids (e.g. valproic acid, phenylbutyric acid), and benzamides [4-9].

The first HDAC inhibitor, suberoylanilide hydroxamic acid (SAHA, Zoinza®), was approved by the U.S. FDA in October 2006 to treat cutaneous T cell lymphoma. Since then, the U.S. FDA has approved three more HDAC inhibitors, including romidepsin (Istodax®), belinostat (PXD101), and panobinostat (LBH-589, Farydak®), for use in clinical settings [7-10]. Most recently, in 2015, chidamide (HBI-8000, tucidinostat, Epidaza®), was approved by the Chinese FDA for relapsed or refractory peripheral T cell lymphoma [11]. A dozen of other HDAC inhibitors, such as mocetinostat (MGCD0103), entinostat (MS-27-527), and givinostat (ITF2357) (Figure 1), are currently undergoing clinical trials for several types of cancer at different phases [12-14]. Except romidepsin, which is naturally occuring, all other compounds are synthetic.

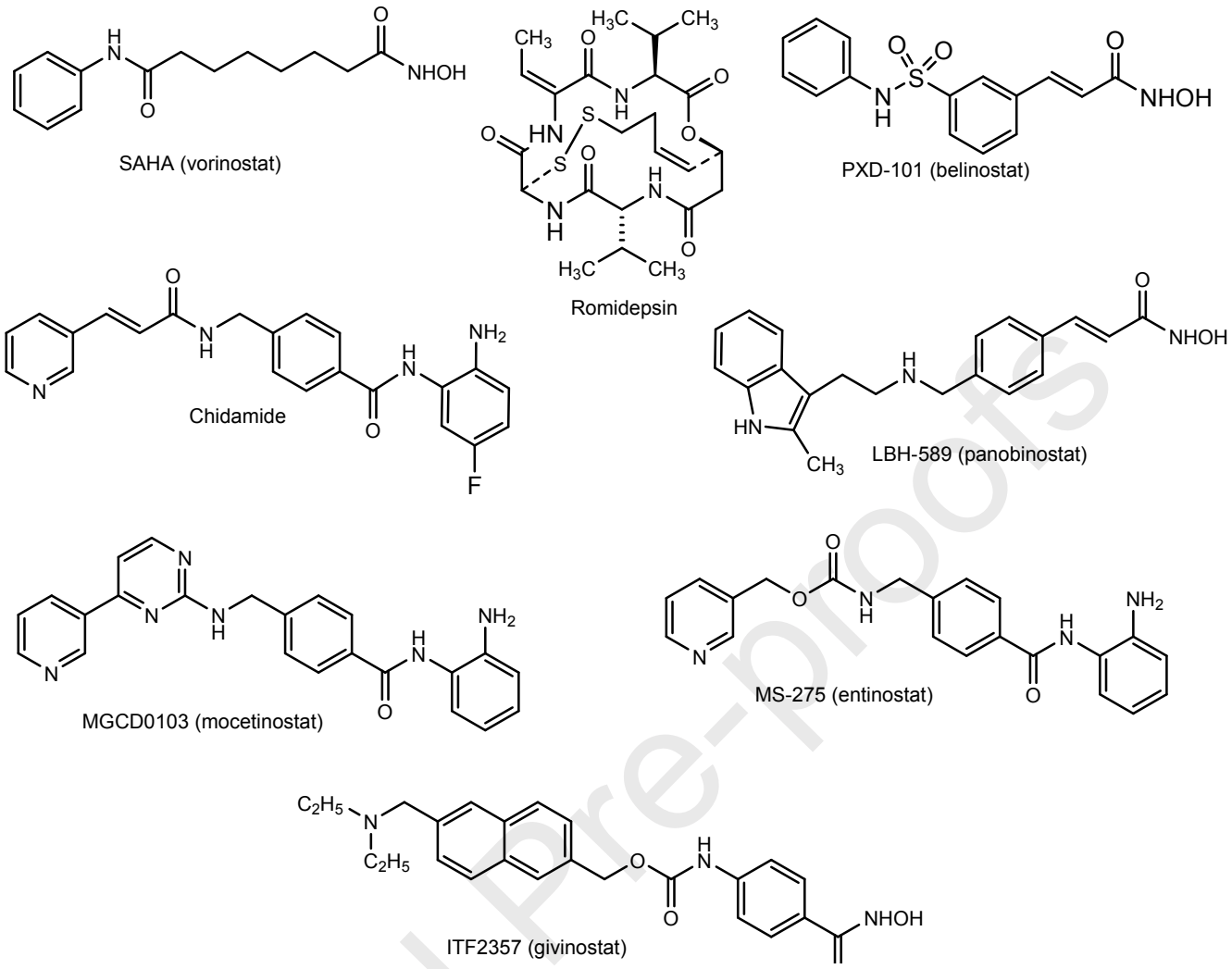

Figure 1. Structures of some HDAC inhibitors approved or under clinical trials

During the last decade, we have explored numerous approaches to discover novel HDAC inhibitors as antitumor agents, including experimental and theoretical methods [15-23]. Several series of heterocycle-based benzothiazole-, 5-aryl-3,4,5-thiadiazole-, or 2-oxoindoline-based hydroxamic acids as analogues of SAHA have been investigated [15-21]. Additionally, some series of *N*-hydroxybenzamides and *N*-hydroxypropenamides as analogues of PXD-101 (belinostat) or ITF2357 (givinostat) have also been synthesized and evaluated for HDAC inhibition and human cancer cell cytotoxicity [20, 21, 24]. All those compound series were found to exhibit very potent HDAC inhibitory activity as well as cytotoxicity [15-23]. Some compounds also exerted *in vivo* antitumor effects in nude mice inoculated inoculated with PC-3 human prostate cancer cells [16]. Continuing our investigation, we expanded our interest into small molecule hydroxamic acids bearing diverse heterocycles such as 1,2-oxazole, 1,3-oxazole indole, pyrazole (Figure 2A). It was expected that the

heterocycles could creat more interaction with the aminoacid chains located in the enzyme active binding site. The results showed that compounds **II**, **VI**, and **VII** displayed significant cytotoxicity and HDAC inhibition in Hela nuclear extract assay (Figure 2A). Of these, compound **II** appeared to be the most promising one. Inspired by these results, we have designed and synthesized several analogues of compound **II** (Figure 2B). This paper describes the results obtained from the synthesis, biological evaluation and docking study of these novel hydroxamic acids bearing 2-benzamido-1,3-oxazole/1,3-thiazole (**5a-g**, **6a-g**) or 2-phenylsulfonamido-1,3-thiazole (**8a-c**).

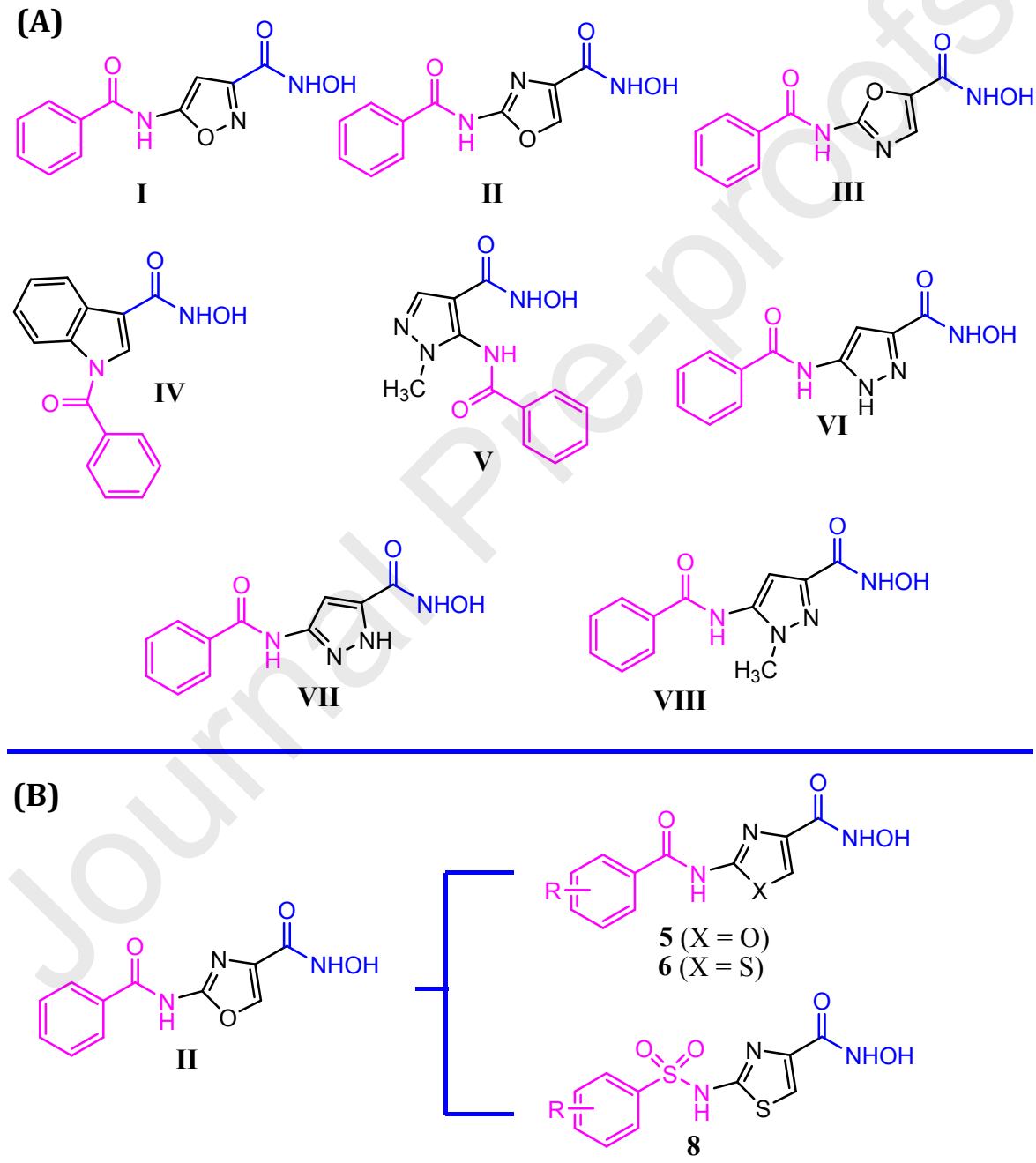

Figure 2. (A) Some small molecule hydroxamic acids bearing 1,2-oxazole, 1,3-oxazole, indole, pyrazole; (B) Rational design of 1,3-oxazole hydroxamic acids as histone deacetylase inhibitors

2. Materials and Methods

2.1. Chemistry

Thin layer chromatography performed using Whatman® 250 μm Silica Gel GF Uniplates and visualized under UV light at 254 and 365 nm, was used to check the progress of reactions and preliminary evaluation of compounds' homogeneity. Melting points were measured using a Gallenkamp Melting Point Apparatus (LabMerchant**,** London, United Kingdom) and were uncorrected. Purification of compounds was carried out using crystallization methods and/or open silica gel column flash chromatography employing Merck silica gel 60 (240 to 400 mesh) as stationary phase. Nuclear magnetic resonance spectra (^{1}H NMR) were recorded on a Bruker 500 MHz spectrometer with DMSO-d_6 as solvent unless otherwise indicated. Tetramethylsilane was used as an internal standard. Chemical shifts are reported in parts per million (ppm), downfield from tetramethylsilane. Mass spectra with different ionization modes including electron ionization (EI), electrospray ionization (ESI), were recorded using PE Biosystems API2000 (Perkin Elmer, Palo Alto, CA, USA) and Mariner® (Azco Biotech, Inc. Oceanside, CA, USA**)** mass spectrometers, respectively. The elemental (C, H, N) analyses were performed on a Perkin Elmer model 2400 elemental analyzer. All reagents and solvents were purchased from Aldrich or Fluka Chemical Corp. (Milwaukee, WI, USA) or Merck unless noted otherwise. Solvents were used directly as purchased unless otherwise indicated.

The synthesis of novel hydroxamic acids bearing 2-benzamidooxazole/thiazole (**5a-g**, **6a-g**) or 2-phenylsulfonamidothiazole (**8a-c)** was carried out as illustrated in Scheme 1. Details are described below.

*General procedures for the synthesis of compounds **5a-g***

To a solution of commercially available ethyl 2-aminooxazole-4-carboxylate (2 mmol) in 10 ml DCM, DMAP (244 mg, 2 mmol) was added. After stirring for 10 minutes, a respective benzoyl chloride (2.2 mmol) was added. The reaction mixture was again stirred at 50℃ for 12 hours. After the reaction was finished (monitored by TLC), the solvent was removed under reduced pressure. A solution of $NaHCO_3$ 5% was gradually added to adjust pH to 7, which led to the formation of white solids. The solids were filtered, washed with cold water and dried at 60℃. The crude product was further purified by column chromatography (DCM/methanol = 95:5) to give the corresponding derivative **3**, yields 67-82%.

Each of the intermediate esters **3** (1 mmol) was dissolved in methanol (10 mL). Then,

hydroxylamine.HCl (685 mg, 10 mmol) was added, followed by dropwise addition of a solution of NaOH (400 mg in 1 mL of water). The mixture was stirred at -5℃ until the reaction completed (1-2 h, checked by TLC). At the end of this reaction, the resulting reaction mixture was poured into ice-cold water, neutralised to pH~7 and acidified by dropwise addition of a solution of HCl 5% to induce the maximum precipitation. The precipitates were filtered, dried and re-crystalised in methanol to give the corresponding target compounds **5a-g**.

*2-Benzamido-N-hydroxyoxazole-4-carboxamide (**5a**)*

White solid; Yield: 65%. mp: 175-176 °C. R_f = 0.47 (DCM : MeOH : AcOH = 90 : 5 : 1). *IR (KBr, cm^{-1}):* 3362 (NH), 3181, 3119 (OH); 3030, 3009 (CH, aren); 1686, 1655 (C=O); 1624, 1599, 1553 (C=C). *^{1}H-NMR (500 MHz, DMSO-d_6, ppm)*: δ 11.67 (1H, s, NHOH), 11.04 (1H, s, CO-NH), 9.11 (1H, s, NHOH), 8.44 (1H, s, H-5), 7.97 (2H, dd, *J* = 8.00 Hz, *J'* = 1.00 Hz, H-2', H-6'), 7.66 (1H, t, *J* = 7.50 Hz, H-4'), 7.56 (2H, t, *J* = 7.75 Hz, H-3', H-5'). *^{13}C NMR (125 MHz, DMSO-d_6, ppm)*: δ 165.92, 158.23, 153.43, 139.09, 134.58, 133.23, 132.93, 129.12, 128.57. *HR-MS (ESI) m/z*: 248.0670 $[M+H]^+$.

*2-(2-Chlorobenzamido)-N-hydroxyoxazole-4-carboxamide (**5b**)*

White solid; Yield: 72%. mp: 191-192 °C. R_f = 0.49 (DCM : MeOH : AcOH = 90 : 5 : 1). *IR (KBr, cm^{-1}):* 3460 (NH); 3254, 3123 (OH); 2982 (CH, aren); 1651 (C=O); 1595, 1557, 1530 (C=C). *^{1}H-NMR (500 MHz, DMSO-d_6, ppm)*: δ 12.12 (1H, s, NHOH), 11.00 (1H, s, CO-NH), 9.30 (1H, s, NHOH), 8.67 (1H, s, H-5), 7.79 (4H, m , H-3', H-4', H-5', H-6'). *^{13}C NMR (125 MHz, DMSO-d_6, ppm)*: δ 163.60, 161.04, 153.44, 142.38, 135.26, 133.06, 132.44, 132.02, 131.08, 129.60, 127.71. *HR-MS (ESI) m/z*: 282.0279 $[M+H]^+$.

*2-(3-Chlorobenzamido)-N-hydroxyoxazole-4-carboxamide (**5c**)*

White solid; Yield: 76%. mp: 193-194 °C. R_f = 0.49 (DCM : MeOH : AcOH = 90 : 5 : 1). *IR (KBr, cm^{-1}):* 3356 (NH); 3156 (OH); 2988, 2872, 2805 (CH, aren); (1686, 1659 (C=O); 1616, 1564 (C=C). *^{1}H-NMR (500 MHz, DMSO-d_6, ppm)*: δ 11.00 (1H, s, CO-NH), 9.11 (1H, s, NHOH), 8.44 (1H, s, H-5), 8.02 (1H, s, H-2'), 7.93 (1H, d , *J* = 7.50 Hz, H-4'), 7.73 (1H, d, *J* = 7.50 Hz, H-6'), 7.59 (1H, t, *J* = 7.75 Hz, H-5'). *^{13}C NMR (125 MHz, DMSO-d_6, ppm)*: δ 164.58, 158.20, 153.48, 138.96, 135.16, 134.54, 133.86, 132.91, 131.09, 128.38, 127.36. *HR-MS (ESI) m/z*: 282.0281 $[M+H]^+$.

*2-(4-Chlorobenzamido)-N-hydroxyoxazole-4-carboxamide (**5d**)*

White solid; Yield: 75%. mp: 198-199 °C. R_f = 0.49 (DCM : MeOH : AcOH = 90 : 5 : 1). *IR (KBr, cm^{-1}):* 3354 (NH); 3156 (OH); 3134, 2988, 2843 (CH, aren); 1690, 1661 (C=O); 1614, 1568 (C=C). *^{1}H-NMR (500 MHz, DMSO-d_6, ppm)*: δ 11.74 (1H, s, NHOH), 11.02 (1H, s, CO-NH), 9.11 (1H, s, NHOH), 8.44 (1H, s, H-5), 7.99 (2H,

d, J = 8.50 Hz, H-2'. H-6'), 7.63 (2H, d, J = 8.50 Hz, H-3', H-5'). *^{13}C NMR (125 MHz, DMSO-d_6, ppm)*: δ 164.96, 158.21, 153.45, 139.03, 138.06, 134.55, 131.84, 130.56, 129.21. *HR-MS (ESI) m/z*: 282.0281 $[M+H]^+$.

*2-(4-Fluorobenzamido)-N-hydroxyoxazole-4-carboxamide (**5e**)*

White solid; Yield: 77%. mp: 179-180 ^{o}C. R_f = 0.45 (DCM : MeOH : AcOH = 90 : 5 : 1). *IR (KBr, cm^{-1}):* 3358 (NH); 3154 (OH); 2988, 2884 (CH, aren); 1686, 1661 (C=O); 1603, 1570, 1504 (C=C). *^{1}H-NMR (500 MHz, DMSO-d_6, ppm)*: δ 11.61 (1H, s, NHOH), 10.92 (1H, s, CO-NH), 9.01 (1H, s, NHOH), 8.35 (1H, s, H-5), 7.97 (2H, dd, J = 8.50 Hz, J' = 5.50 Hz, H-2', H-6'), 7.31 (2H, t, J = 8.75 Hz, H-3', H-5'). *^{13}C NMR (125 MHz, DMSO-d_6, ppm)*: δ 166.19, 164.81, 164.20, 158.23, 153.37, 139.11, 134.58, 131.54, 131.46, 129.44, 116.24, 116.07. *HR-MS (ESI) m/z*: 264.0433 $[M+H]^+$.

*N-Hydroxy-2-(4-methylbenzamido)oxazole-4-carboxamide (**5f**)*

White solid; Yield: 74%. mp: 185-186 ^{o}C. R_f = 0.44 (DCM : MeOH : AcOH = 90 : 5 : 1). *IR (KBr, cm^{-1}):* 3374 (NH); 3161, 3125 (OH); 3042, 2988, 2864 (CH, aren); 1680, 1647 (C=O); 1624, 1551, 1506 (C=C). *^{1}H-NMR (500 MHz, DMSO-d_6, ppm)*: δ 11.46 (1H, s, NHOH), 10.92 (1H, s, CO-NH), 9.01 (1H, s, NHOH), 8.635 (1H, s, H-5), 7.80 (2H, d, J = 7.50 Hz, H-2', H-6'), 7.27 (2H, d, J = 7.50 Hz, H-3', H-5'), 2.31 (3H, s, CH_3). *^{13}C NMR (125 MHz, DMSO-d_6, ppm)*: δ 165.78, 158.26, 153.54, 143.51, 139.11, 134.58, 130.10, 129.64, 128.64, 21.55. *HR-MS (ESI) m/z*: 260.0680 $[M+H]^+$.

*N-Hydroxy-2-(4-methoxybenzamido)oxazole-4-carboxamide (**5g**)*

White solid; Yield: 65%. mp: 181-182 ^{o}C. R_f = 0.43 (DCM : MeOH : AcOH = 90 : 5 : 1). *IR (KBr, cm^{-1}):* 3460, 3368 (NH); 3163, 3121 (OH); 3009, 2847 (CH, aren); 1676, 1651 (C=O); 1597, 1551, 1506 (C=C). *^{1}H-NMR (500 MHz, DMSO-d_6, ppm)*: δ 11.47 (1H, s, NHOH), 11.01 (1H, s, CO-NH), 9.10 (1H, s, NHOH), 8.43 (1H, s, H-5), 7.98 (2H, d, J = 8.50 Hz, H-2', H-6'), 7.08 (2H, d, J = 9.00 Hz, H-3', H-5'), 3.85 (3H, s, OCH_3). *^{13}C NMR (125 MHz, DMSO-d_6, ppm)*: δ 165.25, 163.27, 158.28, 153.67, 139.07, 134.55, 130.71, 124.93, 114.38, 56.02. *HR-MS (ESI) m/z*: 278.0776 $[M+H]^+$.

*General procedures for the synthesis of compounds **6a-g***

Compounds **6a-g** were synthesized via a two-step pathway as illustrated in scheme 1. The procedures were similar to that described for compound **5a-g** with was used commercially available ethyl 2-aminothiazole-4-carboxylate instead of ethyl 2-aminoesters.

*2-Benzamido-N-hydroxythiazole-4-carboxamide (**6a**)*

White solid; Yield: 68%. mp: 189-188 °C. R_f = 0.52 (DCM : MeOH : AcOH = 90 : 5 : 1). *IR (KBr, cm^{-1}):* 3339 (NH); 3262, 3111 (OH); 3057, 2994 (CH, aren); 1655 (C=O); 1601, 1545 (C=C). *^{1}H-NMR (500 MHz, DMSO-d_6, ppm)*: δ 12.64 (1H, s, NHOH), 10.73 (1H, s, CO-NH), 9.05 (1H, s, NHOH), 8.01 (2H, d, *J* = 8.00 Hz, H-2', H-6'), 7.71 (1H, d, *J* = 2.50 Hz, H-5), 7.57 (1H, t, *J* = 7.50 Hz, H-4'), 7.47 (2H, t , *J* = 7.75 Hz, H-3', H-5'). *^{13}C NMR (125 MHz, DMSO-d_6, ppm)*: δ165.98, 159.80, 158.99, 143.72, 133.24, 132.29, 129.12, 128.64, 117.50. *HR-MS (ESI) m/z*: 262.0302 $[M+H]^+$.

*2-(2-Chlorobenzamido)-N-hydroxythiazole-4-carboxamide (**6b**)*

White solid; Yield: 72%. mp: 198-199 °C. R_f = 0.54 (DCM : MeOH : AcOH = 90 : 5 : 1). *IR (KBr, cm^{-1}):* 3337 (NH); 3175, 3117 (OH); 3057, 2967, 2872 (CH, aren); 1680, 1655 (C=O); 1589, 1545 (C=C). *^{1}H-NMR (500 MHz, DMSO-d_6, ppm)*: δ 12.80 (1H, s, NHOH), 10.75 (1H, s, CO-NH), 9.02 (1H, s, NHOH), 7.75 (1H, s, H-5), 7.58-7.37 (4H, m, H-3', H-4', H-5', H-6'). *^{13}C NMR (125 MHz, DMSO-d_6, ppm)*: δ 165.80, 159.56, 158.02, 143.84, 134.65, 132.48, 130.70, 130.24, 129.90, 127.72, 117.88. *HR-MS (ESI) m/z*: 295.9898 $[M+H]^+$.

*2-(3-Chlorobenzamido)-N-hydroxythiazole-4-carboxamide (**6c**)*

White solid; Yield: 74%. mp: 201-202 °C. R_f = 0.54 (DCM : MeOH : AcOH = 90 : 5 : 1). *IR (KBr, cm^{-1}):* 3393 (NH); 3125 (OH); 3065, 2967 (CH, aren); 1651 (C=O); 1599, 1549 (C=C). *^{1}H-NMR (500 MHz, DMSO-d_6, ppm)*: δ 8.07 (1H, d, *J* = 1.50 Hz, H-2'), 7.96 (1H, d, *J* = 8.00 Hz, H-6'), 7.77 (1H, s, H-5), 7.61 (1H, dd, *J* = 8.00 Hz, *J'* = 1.50 Hz, H-4'), 7.49 (1H, t, *J* = 7.75 Hz, H-5'). *^{13}C NMR (125 MHz, DMSO-d_6, ppm)*: δ 164.76, 159.71, 157.59, 143.62, 134.43, 133.90, 132.91, 131.05, 128.48, 127.40, 117.62. *HR-MS (ESI) m/z*: 295.9903 $[M+H]^+$.

*2-(4-Chlorobenzamido)-N-hydroxythiazole-4-carboxamide (**6d**)*

White solid; Yield: 74%. mp: 207-208 °C. R_f = 0.54 (DCM : MeOH : AcOH = 90 : 5 : 1). *IR (KBr, cm^{-1}):* 3395, 3332 (NH); 3142 (OH); 3061, 2968, 2803 (CH, aren); 1651 (C=O); 1593, 1547 (C=C). *^{1}H-NMR (500 MHz, DMSO-d_6, ppm)*: δ 12.75 (1H, s, NHOH), 10.75 (1H, s, CO-NH), 9.07 (1H, s, NHOH), 8.02 (2H, d, *J* = 9.00 Hz, H-2', H-6'), 7.72 (1H, s, H-5), 7.54 (2H, d, *J* = 8.50 Hz, H-3', H-5'). *^{13}C NMR (125 MHz, DMSO-d_6, ppm)*: δ 165.06, 159.74, 158.94, 143.73, 138.11, 131.18, 130.60, 129.22, 117.59. *HR-MS (ESI) m/z*: 295.9905 $[M+H]^+$.

*2-(4-Fluorobenzamido)-N-hydroxythiazole-4-carboxamide (**6e**)*

White solid; Yield: 75%. mp: 188-189 °C. R_f = 0.45 (DCM : MeOH : AcOH = 90 : 5 : 1). *IR (KBr, cm^{-1}):* 3399, 3321 (NH); 3142 (OH); 3075, 2984, 2820 (CH, aren); 1657 (C=O); 1601, 1547, 1510 (C=C). *^{1}H-NMR (500 MHz, DMSO-d_6, ppm)*: δ 12.46 (1H, s, NHOH), 10.73 (1H, s, CO-NH), 9.07 (1H, s, NHOH), 8.10 (2H, dd, *J* = 8.50 Hz, *J'* = 5.50 Hz, H-2', H-6'), 7.73 (1H, s, H-5), 7.31 (2H, t, *J* = 8.75 Hz, H-3', H-

5'). *^{13}C NMR (125 MHz, DMSO-d_6, ppm)*: δ 166.22, 164.92, 164.22, 159.82, 158.95, 143.69, 131.64, 131.57, 128.82, 128.80, 117.47, 116.25, 116.08. *HR-MS (ESI) m/z*: 280.0204 $[M+H]^+$.

*N-Hydroxy-2-(4-methylbenzamido)thiazole-4-carboxamide (**6f**)*

White solid; Yield: 72%. mp: 179-180 °C. R_f = 0.49 (DCM : MeOH : AcOH = 90 : 5 : 1). *IR (KBr, cm^{-1}):* 3447 (NH); 3221 (OH); 3107, 2974, 2903 (CH, aren); 1649 (C=O); 1609, 1541 (C=C). *^{1}H-NMR (500 MHz, DMSO-d_6, ppm)*: δ 12.64 (1H, s, NHOH), 10.70 (1H, s, CO-NH), 9.05 (1H, s, NHOH), 7.92 (2H, d, *J* = 8.50 Hz, H-2', H-6'), 7.70 (1H, s, H-5), 7.27 (2H, d, *J* = 8.00 Hz, H-3', H-5'), 2.30 (3H, s, CH_3). *^{13}C NMR (125 MHz, DMSO-d_6, ppm)*: δ 165.80, 159.88, 159.20, 143.70, 143.55, 129.67, 129.43, 128.69, 117.41, 21.57. *HR-MS (ESI) m/z*: 276.0454 $[M+H]^+$.

*N-Hydroxy-2-(4-methoxybenzamido)thiazole-4-carboxamide (**6g**)*

White solid; Yield: 76%. mp: 197-198 °C. R_f = 0.48 (DCM : MeOH : AcOH = 90 : 5 : 1). *IR (KBr, cm^{-1}):* 3337 (NH); 3215, 3179, 3117 (OH); 2992, 2837 (CH, aren); 1661 (C=O); 1605, 1547, 1501 (C=C). *^{1}H-NMR (500 MHz, DMSO-d_6, ppm)*: δ 12.50 (1H, s, NHOH), 10.67 (1H, s, CO-NH), 9.04 (1H, s, NHOH), 8.02 (2H, d, *J* = 8.50 Hz, H-2', H-6'), 7.69 (1H, s, H-5), 7.00 (2H, d, *J* = 8.50 Hz, H-3', H-5'), 3.77 (3H, s, OCH_3). *^{13}C NMR (125 MHz, DMSO-d_6, ppm)*: δ 165.25, 163.31, 159.92, 159.14, 143.66, 130.78, 124.25, 117.26, 114.42, 56.02. *HR-MS (ESI) m/z*: 294.0539 $[M+H]^+$.

*General procedures for the synthesis of compounds **8a-c***

Compounds **9a-c** were synthesized via a two-step pathway as illustrated in scheme 1. The procedures were similar to that described for compound **6** with was used respective benzenesulfonyl chloride instead of respective benzoyl chloride.

*N-Hydroxy-2-(phenylsulfonamido)thiazole-4-carboxamide (**8a**)*

White solid; Yield: 65%. mp: 193-194 °C. R_f = 0.38 (DCM : MeOH : AcOH = 90 : 5 : 1). *IR (KBr, cm^{-1}):* 3248, 3117 (OH); 3061, 2982, 2905 (CH, aren); 1645 (C=O); 1549 (C=C). *^{1}H-NMR (500 MHz, DMSO-d_6, ppm)*: δ 13.07 (1H, s, NHOH), 11.22 (1H, s, SO_2-NH), 10.86 (1H, s, NHOH), 9.24 (1H, s, H-5), 8.01 (2H, d, *J* = 8.00 Hz, H-2', H-6'), 7.57 (1H, t, *J* = 7.50 Hz, H-4'), 7.47 (2H, d, *J* = 7.75 Hz, H-3', H-5'). *^{13}C NMR (125 MHz, DMSO-d_6, ppm)*: δ 159.13, 156.10, 141.50, 137.44, 129.63, 128.21, 126.36, 111.50. *HR-MS (ESI) m/z*: 297.9965 $[M+H]^+$.

*2-((4-Chlorophenyl)sulfonamido)-N-hydroxythiazole-4-carboxamide (**8b**)*

White solid; Yield: 68%. mp: 221-222 °C. R_f = 0.39 (DCM : MeOH : AcOH = 90 : 5 : 1). *IR (KBr, cm^{-1}):* 3179 (OH); 3098, 2990, 2903 (CH, aren); 1663 (C=O); 1580, 1520 (C=C). *^{1}H-NMR (500 MHz, DMSO-d_6, ppm)*: δ 13.07 (1H, s, NHOH), 11.22 (1H, s, SO_2-NH), 10.86 (1H, s, NHOH), 9.24 (1H, s, H-5), 7.72 (2H, d, *J* = 8.50 Hz, H-2', H-6'), 7.53 (2H, d, *J* = 8.50 Hz, H-3', H-5'). *^{13}C NMR (125 MHz, DMSO-d_6,*

ppm): δ 159.13, 156.09, 141.50, 137.44, 129.63, 128.21, 126.35, 111.50. *HR-MS (ESI) m/z*: 331.9579 $[M+H]^+$.

*N-Hydroxy-2-((4-methylphenyl)sulfonamido)thiazole-4-carboxamide (**8c**)*

White solid; Yield: 66%. mp: 214-215 °C. R_f = 0.42 (DCM : MeOH : AcOH = 90 : 5 : 1). *IR (KBr, cm^{-1}):* 3181, 3127 (OH); 3075, 2974, 2920 (CH, aren); 1649 (C=O); 1595, 1539, 1516 (C=C). *^{1}H-NMR (500 MHz, DMSO-d_6, ppm)*: δ 11.18 (1H, s, SO_2-NH), 10.86 (1H, s, NHOH), 9.24 (1H, s, H-5), 7.60 (2H, s, *J* = 8.00 Hz, H-2', H-6'), 7.26 (2H, d, *J* = 8.50 Hz, H-3', H-5'), 2.27 (3H, s, CH_3). *^{13}C NMR (125 MHz, DMSO-d_6, ppm)*: δ 159.12, 156.19, 142.99, 139.61, 129.93, 129.91, 126.36, 117.65, 21.42. *HR-MS (ESI) m/z*: 312.0122 $[M+H]^+$.

2.2. Biology

2.2.1. Cytotoxicity assay

The cytotoxicity of the synthesized compounds was evaluated against three human cancer cell lines, including SW620 (colon cancer), PC3 (prostate cancer), and NCI-H23 (lung cancer). The cell lines were purchased from a Cancer Cell Bank at the Korea Research Institute of Bioscience and Biotechnology (KRIBB). The media, sera and other reagents that were used for cell culture in this assay were obtained from GIBCO Co. Ltd. (Grand Island, New York, USA). The cells were culture in DMEM (Dulbecco's Modified Eagle Medium) until confluence. The cells were then trypsinized and suspended at 3×10^4 cells/mL of cell culture medium. On day 0, each well of the 96-well plates was seeded with 180 µL of cell suspension. The plates were then incubated in a 5% CO_2 incubator at 37 °C for 24 h. Compounds were initially dissolved in dimethyl sulfoxide (DMSO) and diluted to appropriate concentrations by culture medium. Then 20 µL of each compounds' samples, which were prepared as described above, were added to each well of the 96-well plates, which had been seeded with cell suspension and incubated for 24-h, at various concentrations. The plates were further incubated for 48 h. Cytotoxicity of the compounds was measured by the colorimetric method, as described previously [25] with slight modifications [25-28]. The IC_{50} values were calculated using a Probits software and were averages of three independent determinations (SD ≤ 10%) [29].

2.2.2. HDAC enzymes assay

The HDAC enzymatic assay was performed using a Fluorogenic HDAC Assay Kit (Abcam. MA, USA) according to the manufacturer's instructions. Briefly, HDAC enzymes were incubated with vehicle or various concentrations of the assayed samples or SAHA for 30 min at 37°C in the presence of an HDAC fluorimetric substrate. The HDAC assay developer (which produces a fluorophore in reaction

mixture) was added, and the fluorescence was measured using VICTOR (PerkinElmer, Waltham, MA, USA) with excitation at 360 nm and emission at 460 nm. The measured activities were subtracted by the vehicle-treated control enzyme activities and IC_{50} values were calculated using GraphPad Prism (GraphPad Software, San Diego, CA, USA).

2.2.3. Cell cycle analysis

U937 human lymphoma cells (5×10^5/ml per well) were plated in 6-well culture plates and allowed to grow for 24 h. The cells were treated with compounds at different concentrations for 24 h or 48 h, and then harvested. The harvested cells were washed twice with ice-cold PBS, fixed in 75% ice-cold ethanol, and stained with propidium iodide (PI) in the presence of RNase at room temperature for 30 min. The stained cells were analyzed for DNA content using a FACScalibur flow cytometer (BD Biosciences, San Jose, CA, USA) and the data were processed using Cell Quest Pro software (BD Biosciences).

2.2.4. Apoptosis assay

The Annexin V-FITC/PI dual staining assay was used to determine the percentage of apoptotic cells. U937 cells (5×10^5/ml per well) were plated in 6-well culture plates and allowed to grow for 24 h. The cells were treated with compounds different concentrations for 24 h or 48 h, and then harvested. The harvested cells were washed twice with ice-cold PBS and incubated in the dark at room temperature in 100 ml of 1× binding buffer containing 1 µl Annexin V-FITC and 12.5 mL PI. After 15 min incubation, cells were analyzed for percentage undergoing apoptosis using a FACScalibur flow cytometer (BD Biosciences). The data were processed using Cell Quest Pro software (BD Biosciences).

2.3. Molecular docking studies

The chemical structures of docking compounds were built and energy-optimized within an rms gradient of 0.1 $kcal.mol^{-1}.Å^{-1}$ using MOE 2009.10 package, applying the 94s variant of the Merck Molecular force field (MMFF94s) [30]. The hydroxamic acids were deprotonated taking into account the charge transfer mechanism of HDAC inhibitor [31]. The crystal structure of HDAC enzymes were retrieved from the Protein Data Bank (PDB ID: 4LXZ and 5EEN) [32, 33]. For protein preparation we employed the same procedures reported previously [20, 24]. The flexible-ligand rigid-protein settings were used for docking experiments using MOE Triangle Matcher placement method, keeping 30 poses for conformational analysis. Only conformers that can form bidentate chelation with zinc ion are selected. To

determining binding affinity, London dG scoring (E_score1) and affinity scoring function (E_score2) implemented into MOE 2009.10 were used [30]. The energy minimization using the molecular mechanics force field method was performed for refining the final conformation. Regarding other parameters, default configurations were used.

3. Results and Discussions

3.1. Chemistry

The target hydroxamic acids bearing 2-benzamidooxazole (**5a-g**) or 2-benzamidothiazole (**6a-g**) were obtained straightforwards via a two step pathway, starting from commercially available ethyl 2-aminooxazole-4-carboxylate (**1**) or ethyl 2-aminothiazole-4-carboxylate (**2**). The first step was a simple amidification between compounds **1** and **2** with benzoyl chloride and its different derivatives. The reactions proceeded smoothly in dichloromethane with gentle heating to afford the benzamides **3a-g** and **4a-g** in quantitative yields. The second step involved an acyl nucleophilic substitution between the ester intermediates **3a-g**, **4a-g** and hydroxylamine. The reaction was optimized in methanol. Sodium hydroxide was used as a base to liberate hydroxylamine from its corresponding hydrochloride salt. The second step afforded the target hydroxamic acids **5a-g** and **6a-g** in moderate to good yields.

Three hydroxamic acids bearing 2-phenylsulfonamidothiazole structure (**8a-c)** were reached by a similar two-step pathway, in which benzenesulfonyl chloride or its derivatives were used instead of benzoyl chlorides. All reactions occurred in the same manner.

The structures of the synthesized compounds were determined straightforwardly based on analysis of spectroscopic data, including IR, MS, ^{1}H and ^{13}C NMR.

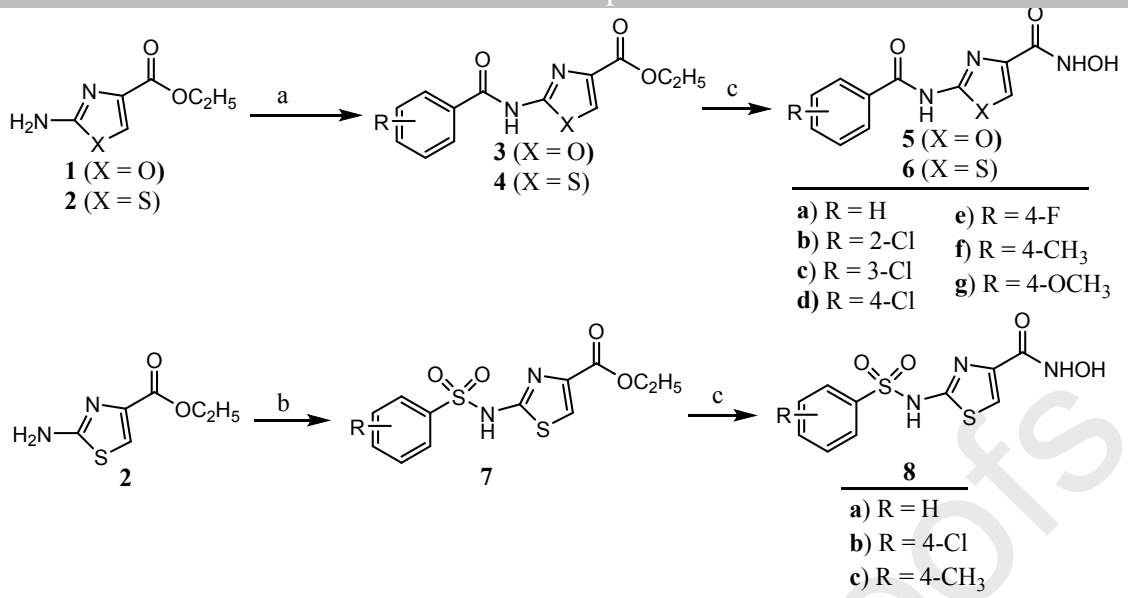

Scheme 1. Synthesis of novel hydroxamic acids bearing 2-benzamidooxazole/thiazole (**5a-g**, **6a-g**) or 2-phenylsulfonamidothiazole (**8a-c)**. Reagents and conditions: a) Benzoyl chloride or its derivatives, DCM, DMAP, 50 ℃; b) $ArSO_2Cl$, DCM, DMAP, 50 ℃; c) H_2N-OH.HCl, NaOH, MeOH.

3.2. Bioactivity

The synthesized compounds were evaluated for their HDAC inhibitory ability using Hela cell nuclear extract assay and cytotoxicity against three human cancer cell lines, including SW620 (colon cancer), PC3 (prostate cancer), and NCI-H23 (lung cancer). SAHA was used as a positive control. The results are presented in Table 1. As shown in Table 1, in general, the synthesized compounds exhibited good cytotoxicity against all three cancer cell lines tested with IC_{50} values of less than 10 μM in all cases. In series **5a-g**, addition of the chloro substitutuent at either positions 2, 3 or 4 of the phenyl ring seemed to slightly enhanced cytoxicity in PC3 cells of the resulting compounds **5b-d** (IC_{50} values, 2.33-3.48 μM), as compared to **5a** (IC_{50} value, 4.35 μM). In almost all other cases, the addition of substituents, either electron releasing (Cl, F) or electron withdrawing groups (CH_3, OCH_3) slightly decreased the cytotoxicity. Generally, however, compounds bearing electron releasing groups (Cl, F) (compounds **5b-e**) were still found to be more potent than compounds bearing electron withdrawing groups (CH_3, OCH_3) (compounds **5f, g**). Compound **5d** could be considered as the most potent in term of cytotoxicity within series **5a-g**. It could be postulated that the presence of halogens would be favorable for the compounds to be more cellular permeable, as manifested by higher logP values. However, other complicate factors, e.g. their electronic influences on the interactions of compounds with HDAC binding site, might also come into play.

Table 1. Inhibition of HDAC activity and cytotoxicity of the synthesized compounds against several cancer cell lines

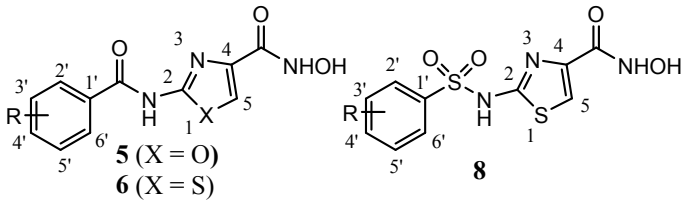

5 (X = O)
6 (X = S)

8

Cpd. code	X	Ar	LogP[1]	HDAC (Hela extract) Inhibition (IC_{50},[2] μM)	Cytotoxicity (IC_{50},[2] μM)/Cell lines[3]		
					SW620	PC3	NCI-H23
5a	O	H	0.16	0.068±0.012	1.98±0.13	4.35±0.58	3.29±0.20
5b	O	2-Cl	0.80	0.056±0.010	2.31±0.14	2.33±0.05	4.92±0.30
5c	O	3-Cl	0.80	0.029±0.003	3.22±0.39	3.35±0.10	3.79±0.43
5d	O	4-Cl	0.80	0.069±0.011	2.40±0.05	3.48±0.01	2.70±0.23
5e	O	4-F	0.36	0.038±0.001	5.36±0.39	5.44±0.86	5.80±0.77
5f	O	4-CH_3	0.71	0.010±0.001	6.68±0.91	5.11±0.10	3.87±0.46
5g	O	4-OCH_3	0.24	0.069±0.003	3.43±0.38	7.50±0.91	5.65±0.53
6a	S	H	1.07	0.037±0.002	4.22±0.17	8.48±1.11	6.14±0.27
6b	S	2-Cl	1.72	0.051±0.001	5.99±0.48	3.78±0.53	7.69±0.83
6c	S	3-Cl	1.72	0.038±0.007	3.02±0.20	5.02±0.82	5.02±0.37
6d	S	4-Cl	1.72	0.033±0.001	4.42±0.56	6.57±0.50	6.78±0.23
6e	S	4-F	1.27	0.035±0.002	3.47±0.21	4.64±0.43	6.24±0.02
6f	S	4-CH_3	1.62	0.131±0.052	2.21±0.01	4.34±0.64	3.29±0.51
6g	S	4-OCH_3	1.15	0.073±0.009	6.54±0.01	6.05±0.08	6.41±0.08
8a	S	H	0.25	0.059±0.006	2.28±0.07	2.11±0.09	1.57±0.05
8b	S	4-Cl	0.90	0.036±0.0	2.17±0.	1.96±0.	1.45±0.10

8c	S	4-CH_3	0.33	04 0.044±0.000	15 1.91±0.18	01 2.24±0.34	1.73±0.08
SAHA[4]		264.32	1.44	0.025±0.002	1.12±0.10	1.82±0.09	1.44±0.17

[1]*Calculated by KOWWIN v1.67 software;* [2]*The concentration (μM) of compounds that produces a 50% reduction in enzyme activity or cell growth, the numbers represent the averaged results from triplicate experiments;* [3]*Cell lines: SW620, colon cancer; PC3, prostate cancer; NCI-H23, lung cancer;* [4]*SAHA, suberoylanilide acid, a positive control.*

Thiazole compounds (series **6a-g**) seemed to be slightly less potent than the oxazole ones (series **5a-g**) in term of cytotoxicity. It was hard to delineate the structure-cytotoxicity relationships within series **6a-g**. In this series, compound **6g** bearing 4-methoxy substituent on the phenyl ring appeared to be the most cytotoxic one, but still less potent than SAHA. Noteworthy, three compounds of sulfonamide type (**8a-c**) exhibited stronger cytotoxicity compared to benzamide compounds (series **5a-g, 6a-g**). The cytotoxicity of compounds **8a-c** was comparable to that of SAHA. These results suggest the sulfonamide functionality appears to be more favorable for the bioactivity of these compound types and further exploration of the hydroxamic acids incorporating sulfonamide functionality similar to compounds **8a-c** should warranted.

Regarding the HDAC inhibition, compounds **5a, 6a** and **8a** dislayed potent activity with IC_{50} values being 0.068, 0.037 and 0.059 μM, respectively. Generally, in series **5a-g** introduction of the substituents on the phenyl ring of the benzamide moeity retained or in some cases even enhanced the HDAC inhibitory activity. Compound **5f** bearing 4-methyl substituent was the most potent HDAC inhibitor with IC_{50} value as low as 0.010 μM. In series **6a-g**, a clearer structure-HDAC inhibition relationship was observed. Electron-withdrawing substituents seemed to retain or enhance the HDAC inhibitory activity (such as -Cl, compounds **6c, 6d**, IC_{50} values 0.038, 0.033 μM), respectively, meanwhile, electron-releasing substituents (such as -CH_3, -OCH_3, compounds **6f, 6g**, IC_{50} values 0.252, 0.628 μM).

Although generally less potent than SAHA, based on the IC_{50} values, these compounds were still very potent in term of HDAC inhibition. And given their structral simplicity, further investigation of this type of compounds should be warranted.

The results from SRB assays demonstrate that the compounds in three series **5a-g, 6a-g** and **8a-c** displayed relatively potent cytotoxicity against three human cancer cell lines. We next decided to investigate whether these compounds affect the cell cycle

and apoptosis. Three representative compounds, including **5a, 6a** and **8a**, were selected and the flow cytometry was used to analyze the effects of compounds on the cell cyle. SW620 human colon cancer cells were treated with each compound at different concentrations for 24 h and then DNA contents were analyzed. It was found that, at 10 μM, all compounds did not affect the cell cycle (Figure 3A). At 50 μM, compounds **5a, 6a** and **8a** mainly increased the cell death population (7.08, 15.55, and 15.83%, respectively, vs. 6.69% of the VH, Figure 3B), while their effects on other phases of the cell cycle were still not clearly observable. We decided to increase the compounds concentration to 100 μM and found that, at this concentration, compounds **6a** and **8a** significantly arrested cells at G2 phase of the cell cycle (20,53 and 26.99%, respectively, vs. 6.21% of the VH, Figure 3C).

Next, to investigate whether the compounds induce apoptosis we used an Annexin V-FITC/propidium iodide (PI) dual staining assay. Three representative compounds, including **5a, 6a** and **8a** were chosen. Phosphatidylserine (PS) is one component of the cell membrane which plays a key role in cell cycle signaling, especially in relation to apoptosis. During early apoptosis, PS, which locates on the cytosolic (inner) side of the cell membrane, translocates to the extracellular (outer) surface of the cell membrane. Propidium iodide (PI) is a fluorescent intercalating agent. Normally, the membrane of live cells is not permeable to PI. However, the membrane of dead cells or cells in the latter stages is permeable to PI and their nuclei stain red. Annexin V intrinsically has a high affinity for PS, therefore, annexin V fluorescently labelled with fluorescein isothiocyanate (FITC) has been used to identify early apoptotic cells. We treated SW620 cells with different concentrations of compounds **5a, 6a** and **8a** for 24 h, then stained the cells with Annexin V-FITC and PI. The results illustrated in Figure 4 show that, at 10 μM, all three compounds did not affect the cell cycle (Figure 4A). At 50 μM, compounds **6a** and **8a** slightly increased the early apoptotic cell population (Figure 4B). However, at 100 μM concentration, the induction of both early and late apoptosis in SW620 cells was clearly observed with compounds **6a** and **8a** (Figure 4C).

Consistent with the effects on the cell cycle and apoptosis, compounds **6a** and **8a** at 50 μM concentration also significantly caused morphological changes of SW620 cells (Figure 5A). These effects were much more pronounced at higher concentration of 100 μM (Figure 5B).

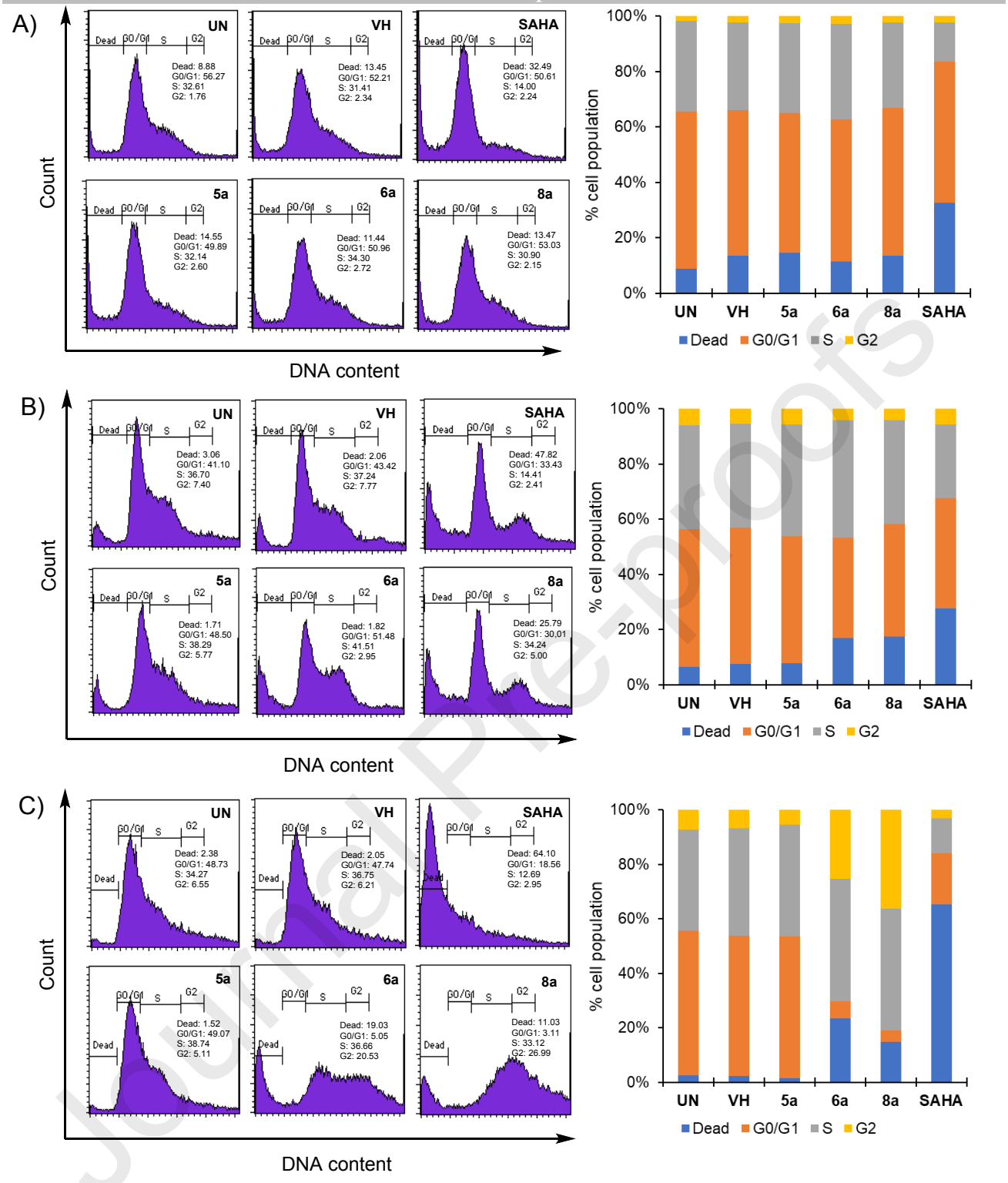

Figure 3. Cell cycle analysis of representative compounds **5a, 6a** and **8a**. SW620 (human colon cancer) cells (5 x 10^5 cells/well in 6-well plate, pre-incubated for 2 h) were treated with compounds (10 μM) and SAHA (10 μM) for 24 h (A). SW620 (human colon cancer) cells (2 x 10^5 cells/well in 6-well plate, pre-incubated for 2 h) were treated with compounds (50 μM) and SAHA (1 μM) for 24 h (B). SW620 (human colon cancer) cells (2 x 10^5 cells/well in 6-well plate, pre-incubated for 24 h) were treated with compounds (100 μM) and SAHA (10 μM) for 48 h (C). The harvested cells were stained with propidium iodide (PI) in the presence of RNase and

then were analyzed for DNA content. UN: untreated, VH: vehicle (DMSO. 0.05%).

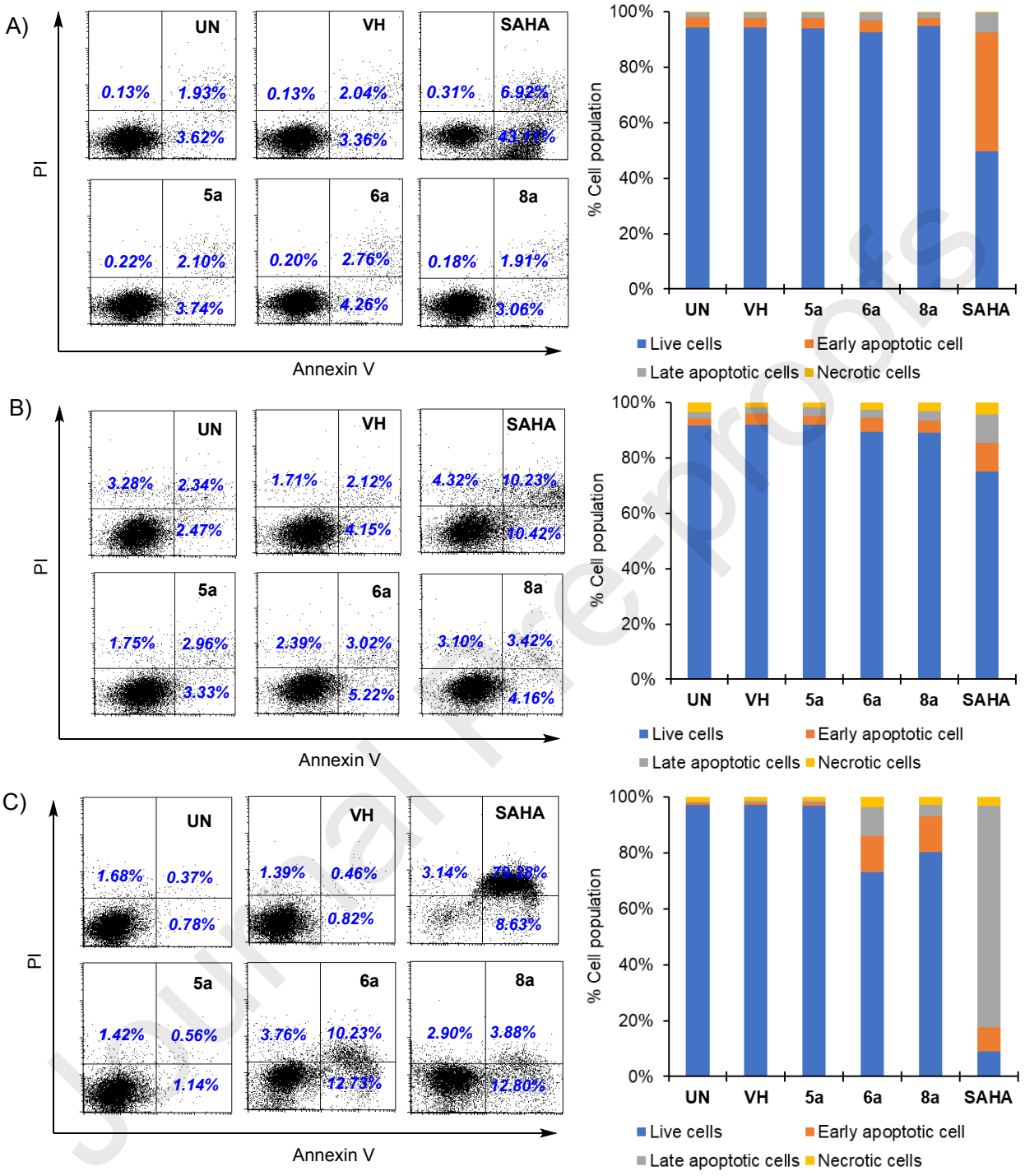

Figure 4. Apoptosis **(Annexin V/PI)** analysis of representative compounds **5a, 6a** and **8a**. SW620 (human colon cancer) cells (5 x 10^5 cells/well in 6-well plate, pre-incubated for 2 h) were treated with compounds (10 μM) and SAHA (10 μM) for 24 h (A). SW620 (human colon cancer) cells (2 x 10^5 cells/well in 6-well plate, pre-incubated for 2 h) were treated with compounds (50 μM) and SAHA (1 μM) for 24 h (B).SW620 (human colon cancer) cells (2 x 10^5 cells/well in 6-well plate, pre-incubated for 24 h) were treated with compounds (100 μM) and SAHA (10 μM) for

48 h (C). The harvested cells were incubated with Annexin V-FITC and PI. UN: untreated, VH: vehicle (DMSO. 0.05%). Area 1 = PI positive population, Area 2: Annexin V-postivie population.

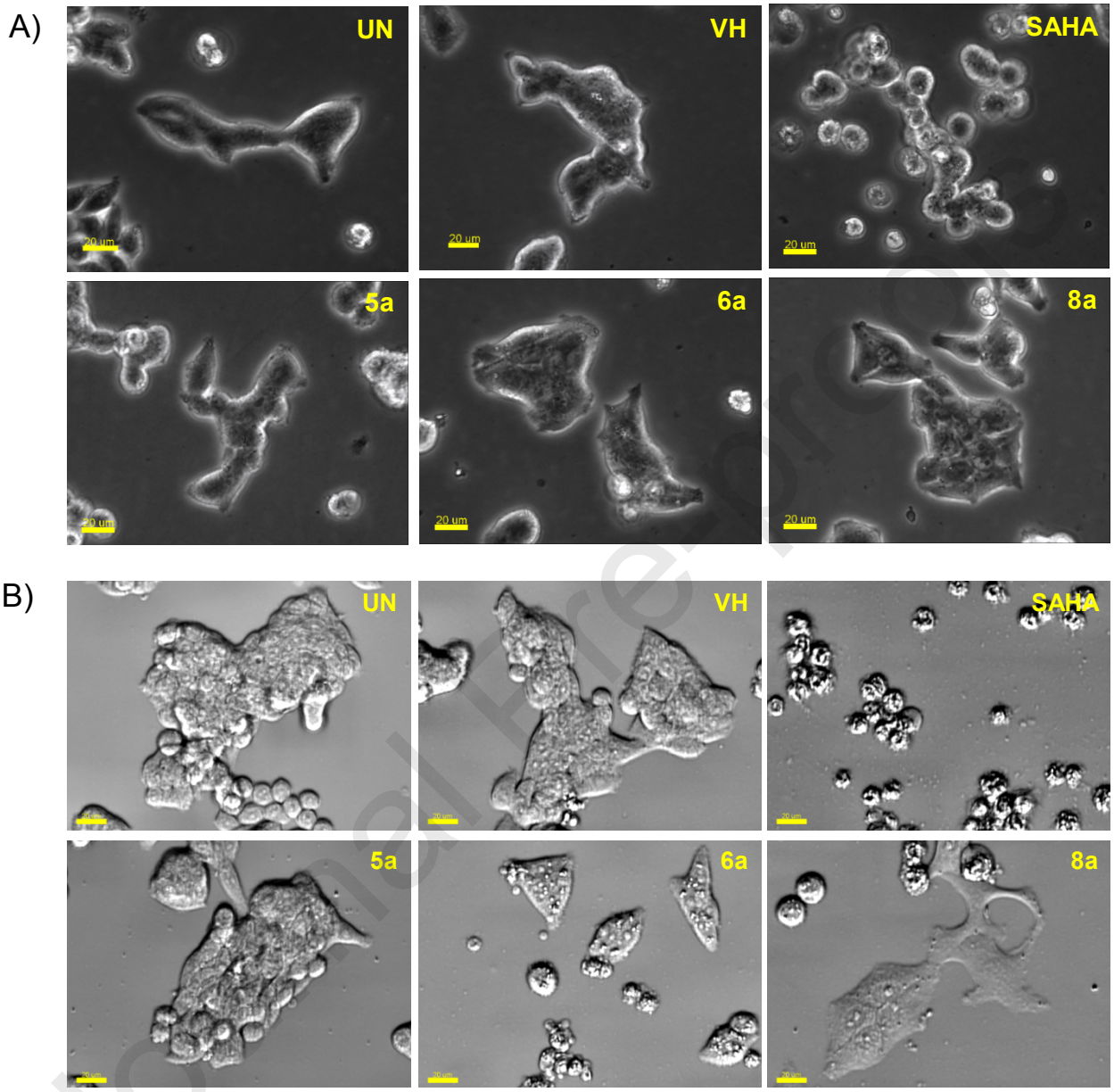

Figure 5. Morphology changes of cells treated with representative compounds **5a, 6a** and **8a** or SAHA. SW620 (human colon cancer) cells (2 x 10^5 cells/well in 6-well plate, pre-incubated for 2 h) were treated with compounds (50 μM) and SAHA (1 μM) for 24 h (A). SW620 (human colon cancer) cells (2 x 10^5 cells/well in 6-well plate, pre-incubated for 24 h) were treated with compounds (100 μM) and SAHA (10 μM) for 48 h (B). Then, the cells were photographed using an Imaging Device: Biostation with 40X lens. Scale bar: 20 μm.

3.3. Molecular docking studies

In order to further explore the structure-activity relationship of HDAC inhibition activity of synthesized compounds, docking simulations were carried out using MOE software. To do so, two crystal structures of HDAC enzymes were selected: (i) HDAC2 in complex with SAHA (PDB ID: 4LXZ) [32], and (ii) HDAC6 in complex with Belinostat (PDB ID: 5EEN) [33] which shares similar structure features with our designed compounds. By using two isozymes of different classes (HDAC2 belongs to class I meanwhile HDAC6 class IIB) we could reveal some evidences related to the selectivity of synthesized compounds.

Firstly, the docking procedures were validated by redocking the co-crystal ligand the active site of the enzymes. For HDAC2, the redocked and co-crystal SAHA conformations were highly superimposed with RMSD = 0.3770Å. As can be observed in Figure 6A, the key H-bonding interactions with the residues Asp104, His145, His146 and Tyr308 were well conserved. In addition, the hydroxamic group of the redocked SAHA formed typical bidentate chelation with the cofactor zinc ion in the binding site which is the key element of the experimental binding model. According HDAC6, we also obtained good docking results. The deviation between redocked and co-crystal binding poses was quite low (RMSD = 0.8103Å). All the key interactions with His573, His574, Phe643 and Tyr745 were conserved (see Figure 6B). The hydroxamate group of Belinostat also formed stable chelate complex with zinc ion of HDAC6. The docking scores calculated for redocked SAHA and Belinostat were shown in Table 2. From the results obtained, we can conclude that the currently applied docking protocols are suitable for using in the subsequent docking studies.

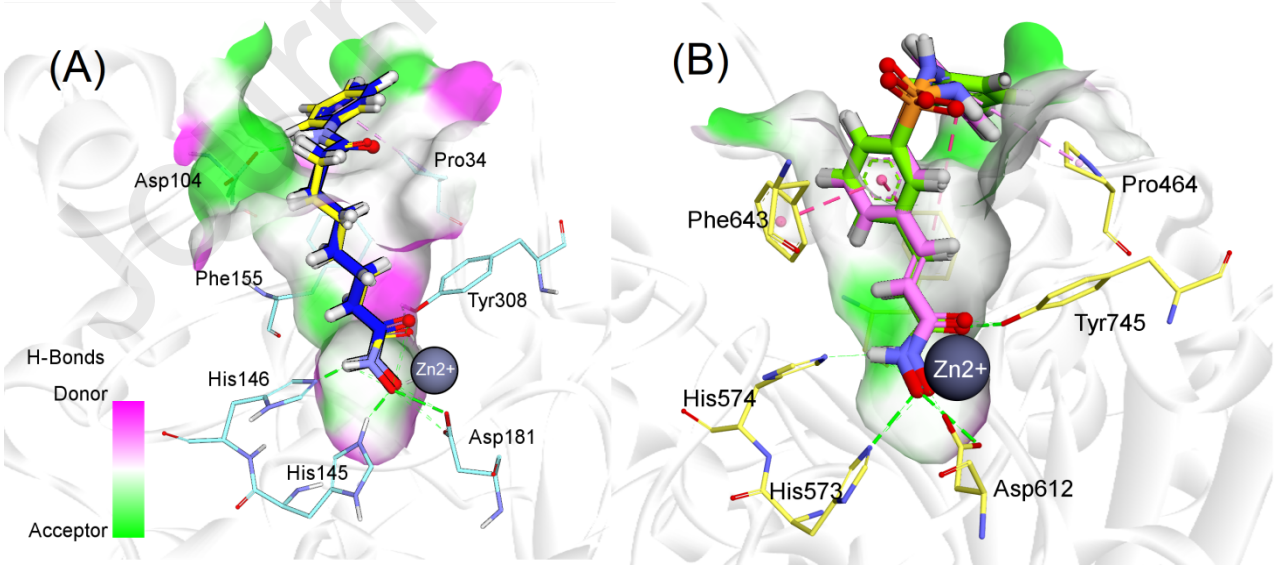

Figure 6. Superposition between: (A) redocked (blue) and co-crystal (yellow) SAHA in HDAC2 (PDB ID: 4LXZ), and (B) redocked (pink) and co-crystal (green)

Belinostat in HDAC6 (PDB ID: 5EEN). The binding pockets are colored by hydrogen bond type.

In the next steps, all the 17 synthesized compounds (**5a-g**, **6a-g**, **8a-c**) were docked into the binding site of HDAC2 and HDAC6 enzymes. Most of the HDAC inhibitors conform to a Cap-Linker-Chelator pharmacophoric model [31, 34]. The cap group can interact with the external surface of the active site, connecting with the zinc binding group (chelator) through a linker that accommodate the tubular access of the active site [6]. Our compounds were mainly designed based the modifications made on the 1,3-oxazole and 1,3-thiazole rings of the linker groups. This substitution might affect the interactions with the residues in the long tunnel in the HDAC pocket. For HDAC2, all the compounds formed multiple pi-stacking interactions with Phe155, His183 and Phe210 which is different from that of SAHA, meanwhile the key H-bonding interactions are similar to SAHA. As can be seen in the Figure 6B, all the compounds were well accomodated in the binding site of HDAC2 and formed bidentate chelation with zinc ion in the same fashion of redocked SAHA. Table 2 showed the similarly close distances (1.95-2.73Å) between hydroxamate groups and zinc ion of all the compounds.

Likewise, all compounds were found to be lying deep into the binding pocket of HDAC6. They could form chelation with zinc ion in the same manner of Belinostat. With exception of **5c**, **6b** and **6f**, compounds **5a-g** and **6a-g** formed three H-bonds with His573, His574, and Gly582. Meanwhile compounds **8a-b** have additional H-bond between sulfonyl group of linker with His614. As can be observed in the Table 2, the docking scores calculated for lingands in complexes with HDAC6 were slightly lower than HDAC2, suggesting the higher affinity of synthesized compounds towards HDAC6 compared to HDAC2 isozyme.

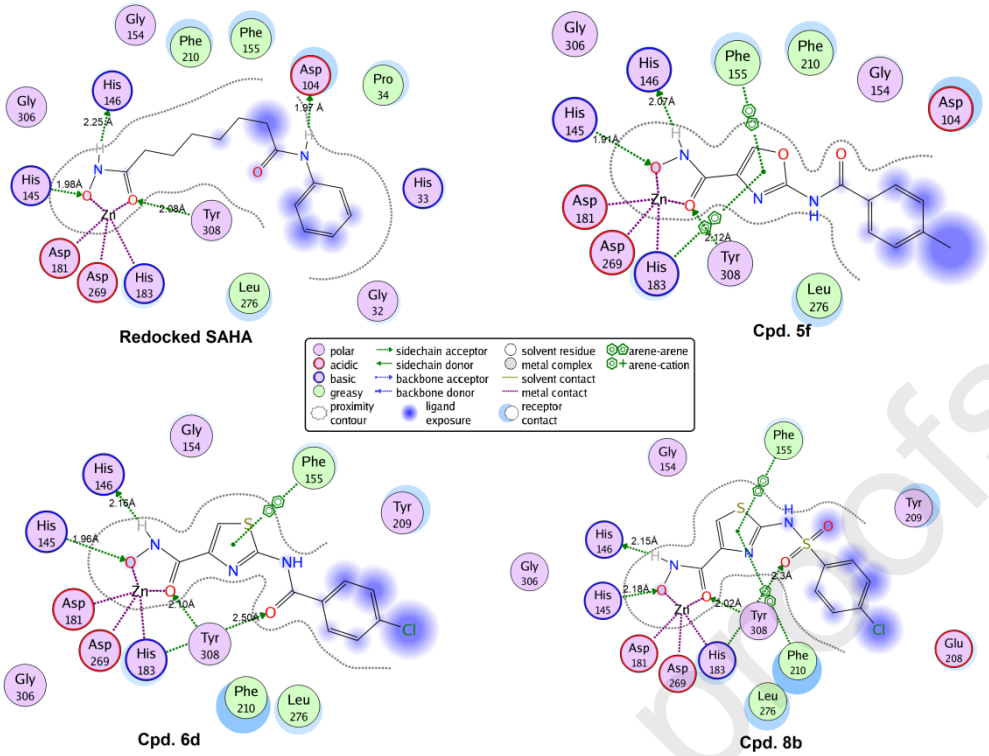

Figure 7. Topological presentation of the binding modes and interactions of compounds SAHA (redocked), **5f**, **6d**, and **8b** in HDAC2 active site.

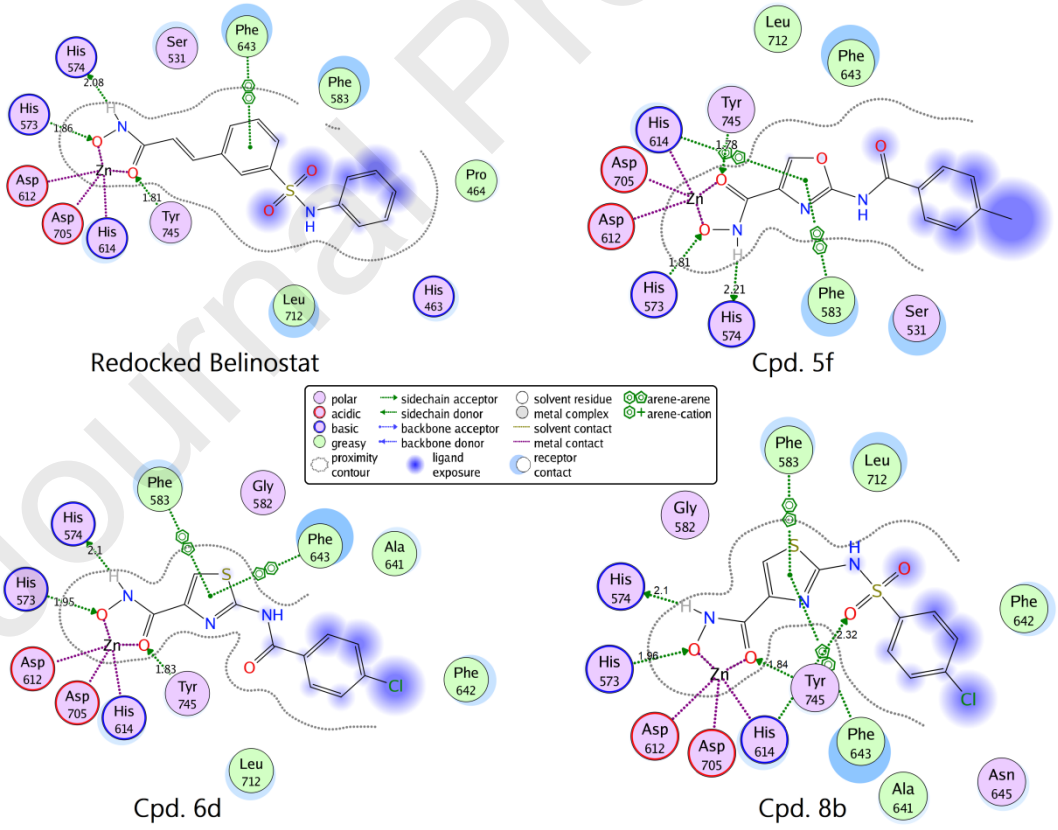

Figure 8. Topological presentation of the binding modes and interactions of compounds Belinostat (redocked), **5f**, **6d**, and **8b** in HDAC6 active site.

Figure 7 and 8 illustrates the comparison between the binding modes of some representative compounds (**5f**, **6d**, **8b**) and reference compounds (SAHA and Belinostat). These compounds are the most potential compounds according to HDAC inhibition from each series. For HDAC2, all the compounds could form 3 to 4 H-bonding interactions with His145, His146, His183 and Tyr308 (Figure 7). The van der Waals interactions involved in holding ligands within the active site include pi-interactions between the 1,3-oxazole and 1,3-thiazole linker moieties and aromatic rings of Phe155, His183 and Phe210. In addition, the capping group showed numerous interactions with residues at the rim of the pocket, such as Asp104, Tyr209 and Leu276. Recently, we have investigated the N-hydroxybenzamide scaffold as linker and observed very similar results to those obtained in this study [20, 24, 35]. On the other hand, the interactions between three synthesized compounds were quite similar to Belinostat. As can be reveal in Figure 8, the pi-stacking interactions with hydrophobic residues Phe583 and Phe643 appeared to be important for stabilizing the ligand-protein complexes. In addition compound **8b** showed higher H-bonding interactions with HDAC6 compared to Belinostat, **5f** and **6d**. Considering the importance of isoform selectivity, especially to avoid cardiac side effects in screening novel HDAC inhibitors, it would be of high interest to experimentally investigate the inhibitory selectivity of our synthesized compounds towards HDAC enzymes in the future.

We continued analyzing the correlations between the docking scores and the IC_{50} values. Our scoring calculations were based on two common function applied in the MOE package, including the London and affinity scoring functions. As can be seen in Figure 8, for both systems (HDAC2 and HDAC6), the binding affinities calculated via London scoring function showed higher correlation with experimental values (R^2 = 0.76 and 0.71) compared to that calculated using other method (R^2 = 0.65 and 0.61). These findings agreed with previous results and once again confirmed the ability of London scoring function to quantitatively predict the experimental HDAC inhibitory activity [24].

Table 2. Docking scores of all compounds with HDAC2 and HDAC6 enzymes.

Cpd. code	**HDAC2**				**HDAC6**			
	E_Score1*	**E_score2***	**Distance to Zn^{2+}***		**E_Score 1**	**E_score 2**	**Distance to Zn^{2+}**	
			-OH	**=O**			**-OH**	**=O**
5a	-14.535	-7.005	1.97	2.34	-15.737	-9.516	1.95	2.4

5b	-16.471	-7.435	2.01	2.3	-15.901	-9.425	1.94	2.46
5c	-17.872	-8.851	1.96	2.32	-18.671	-10.438	1.95	2.48
5d	-14.772	-6.966	1.95	2.39	-15.945	-9.607	1.95	2.41
5e	-15.463	-7.126	1.96	2.33	-17.974	-9.513	1.95	2.41
5f	-19.695	-9.430	1.97	2.34	-20.014	-10.974	2.07	2.21
5g	-15.442	-7.149	1.96	2.32	-17.308	-9.869	1.95	2.38
6a	-16.404	-7.521	1.96	2.43	-17.269	-9.732	1.95	2.38
6b	-18.134	-7.783	1.97	2.47	-17.266	-9.887	1.95	2.37
6c	-16.261	-7.483	2.04	2.47	-17.391	-9.846	1.95	2.37
6d	-17.190	-8.122	2.03	2.43	-17.768	-9.971	1.96	2.47
6e	-16.958	-8.058	1.97	2.47	-16.518	-9.901	1.96	2.48
6f	-12.592	-6.834	1.98	2.48	-13.674	-9.482	2.02	2.31
6g	-13.644	-7.111	1.97	2.48	-14.814	-9.772	1.95	2.36
8a	-15.085	-7.791	1.99	2.45	-18.328	-10.071	1.95	2.52
8b	-17.921	-8.958	1.96	2.73	-16.960	-10.259	1.95	2.48
8c	-15.479	-7.493	1.98	2.60	-16.165	-10.189	1.99	2.23
SAHA	-19.102	-7.757	1.96	2.54				
Belinostat					-19.030	-10.885	1.96	2.30

* The docking score (kcal/mol) calculated from the London (with refinement) and affinity scoring function from MOE software

** Distances (Å) from oxygen atoms (-O and =OH) of hydroxamate group to zinc ion.

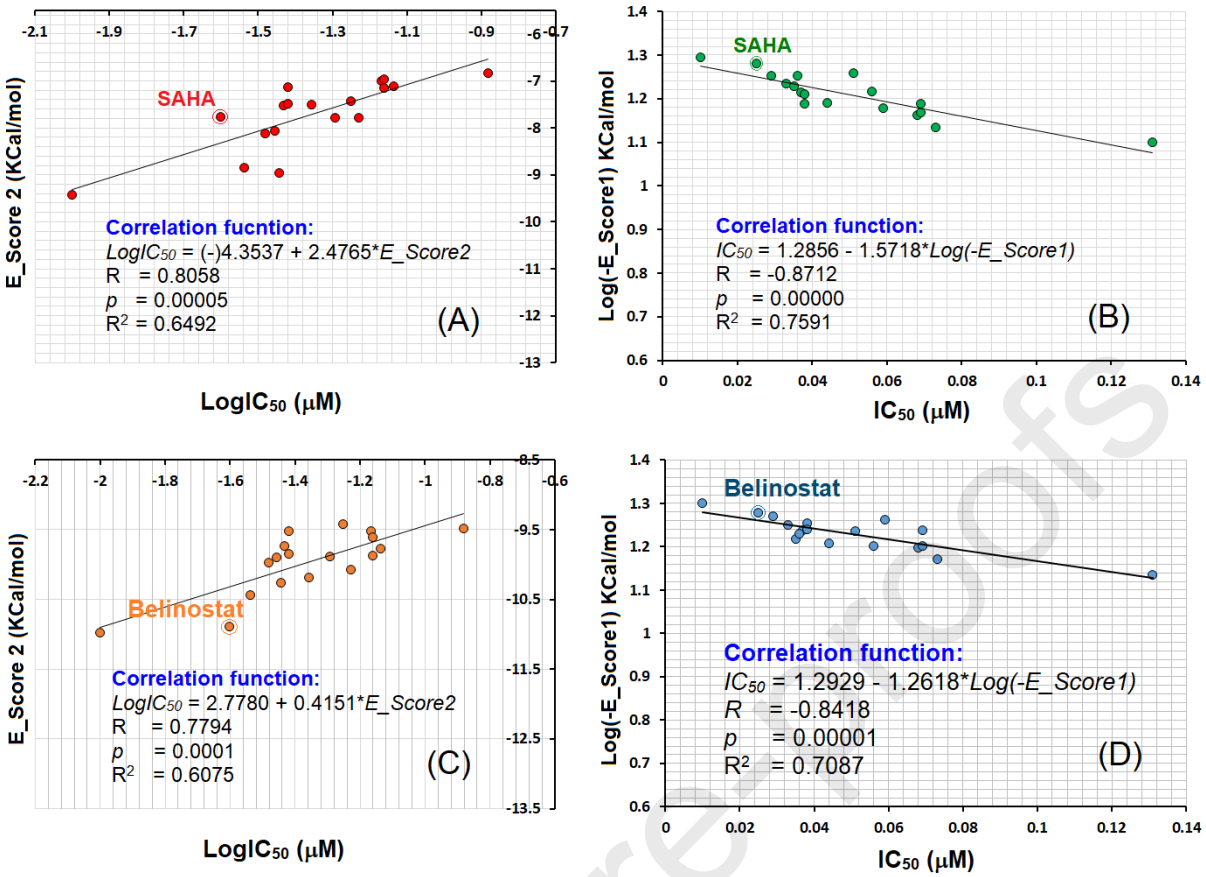

Figure 9. Correlation analysis of IC_{50} values and docking scores determined for all the ligands bound to HDAC2 (A-B) and HDAC6 (C-D).

4. Conclusions

In conclusion, we have reported here seventeen simple hydroxamic acids bearing 1,3-oxazole- and 1,3-thiazole scallfods and evaluated their cytotoxicity as well as their HDAC inhibition. Overall, the compounds were potent HDAC inhibitors. Some compounds (with IC_{50} values as low as 0.010 μM) were even more potent than SAHA. These compounds also exhibited good cytotoxicity with IC_{50} values in a range from 1.45 to 7.69 μM. Representative compounds **6a** and **8a** appeared to arrest the SW620 cell cycle at G2 phase and significantly induced both early and late apoptosis of SW620 colon cancer cells. Docking experiments on HDAC2 and HDAC6 isozymes revealed some pi-stacking interactions formed between the 1,3-oxazole and 1,3-thiazole linker moieties toward hydrophobic residues at the tunnel of the HDAC active site which positively contributed to the inhibitory activity of synthesized compounds. The binding affinity predicted by docking program showed good correlation with the experimental IC_{50} values. This study demonstrates that simple 1,3-oxazole- and 1,3-thiazole-based hydroxamic acids are also promising as

antitumor agents and HDAC inhibitors. Also, these results should provide valuable information for further design of more potent HDAC inhibitors and antitumor agents.

Acknowledgements

We acknowledge the principal financial supports from the National Foundation for Science and Technology of Vietnam (NAFOSTED, Grant number 104.01-2017.301). The work was also partly supported by a grant funded by the Korean Government (NRF-2017R1A5A2015541) for more indepth-biological evaluation and mechanism study.

Declaration of interest

The authors declarate no conflict of interest.

References

[1] C. A. Hamm, F. F. Costa, 'Epigenomes as therapeutic targets', *Pharmacol. Ther.* **2015**, *151*, 72-86.

[2] A. J. M. Ruijter, A. H. Gennip, H. N. Caron, S. Kemp, A. B. P. Kuilenburg, 'Histone deacetylases (HDACs): characterization of the classical HDAC family', *Biochem. J.* **2003**, *370*, 737-749.

[3] O. Witt, H. E. Deubzer, T. Milde, I. Oehme, 'HDAC family: What are the cancer relevant targets?', *Cancer Lett.* **2009**, *277*, 8-21.

[4] K. Ververis, A. Hiong, T. C. Karagiannis, P. V. Licciardi, 'Histone deacetylase inhibitors (HDACIs): multitargeted anticancer agents', *Biologics.* **2012**, *7*, 47-60.

[5] S. Valente, A. Mai, 'Small-molecule inhibitors of histone deacetylase for the treatment of cancer and non-cancer diseases: a patent review (2011 – 2013)', *Expert Opin. Ther. Pat.* **2014**, *24*, 401-415.

[6] L. Jiyang, L. Guangqiang, X. Wenqing, 'Histone Deacetylase Inhibitors: An Attractive Strategy for Cancer Therapy', *Curr. Med. Chem.* **2013**, *20*, 1858-1886.

[7] C. Zwergel, S. Valente, C. Jacob, A. Mai, 'Emerging approaches for histone deacetylase inhibitor drug discovery', *Expert Opin. Drug Discov.* **2015**, *10*, 599-613.

[8] A. C. West, R. W. Johnstone, 'New and emerging HDAC inhibitors for cancer treatment', *J. Clin. Invest.* **2014**, *124*, 30-39.

[9] J. E. Bolden, M. J. Peart, R. W. Johnstone, 'Anticancer activities of histone deacetylase inhibitors', *Nat. Rev. Drug Discov.* **2006**, *5*, 769-784.

[10] S. P. Iyer, F. F. Foss, 'Romidepsin for the Treatment of Peripheral T-Cell Lymphoma', *Oncologist.* **2015**, *20*, 1084-1091.

[11] M. Guha, 'HDAC inhibitors still need a home run, despite recent approval', *Nat. Rev. Drug Discov.* **2015**, *14*, 225-226.

[12] T. Qiu, L. Zhou, W. Zhu, T. Wang, J. Wang, Y. Shu, P. Liu, 'Effects of treatment with histone deacetylase inhibitors in solid tumors: a review based on

30 clinical trials', *Future Oncol.* **2013**, *9*, 255-269.
[13] T. U. Bracker, A. Sommer, I. Fichtner, H. Faus, B. Haendler, H. Hess-Stumpp, 'Efficacy of MS-275, a selective inhibitor of class I histone deacetylases, in human colon cancer models', *Int. J. Oncol.* **2009**, *35*, 909-920.
[14] K. B. Glaser, 'HDAC inhibitors: Clinical update and mechanism-based potential', *Biochem. Pharmacol.* **2007**, *74*, 659-671.
[15] D. T. K. Oanh, H. V. Hai, S. H. Park, H.-J. Kim, B.-W. Han, H.-S. Kim, J.-T. Hong, S.-B. Han, V. T. M. Hue, N.-H. Nam, 'Benzothiazole-containing hydroxamic acids as histone deacetylase inhibitors and antitumor agents', *Bioorg. Med. Chem. Lett.* **2011**, *21*, 7509-7512.
[16] T. Truong Thanh, O. Dao Thi Kim, D. Phan Thi Phuong, H. Van Thi My, P. Sang Ho, H. Byung Woo, K. Youngsoo, H. Jin-Tae, H. Sang-Bae, N. Nguyen-Hai, 'New Benzothiazole/thiazole-Containing Hydroxamic Acids as Potent Histone Deacetylase Inhibitors and Antitumor Agents', *Med. Chem.* **2013**, *9*, 1051-1057.
[17] N.-H. Nam, T. L. Huong, D. T. M. Dung, P. T. P. Dung, D. T. K. Oanh, S. H. Park, K. Kim, B. W. Han, J. Yun, J. S. Kang, Y. Kim, S.-B. Han, 'Synthesis, bioevaluation and docking study of 5-substitutedphenyl-1,3,4-thiadiazole-based hydroxamic acids as histone deacetylase inhibitors and antitumor agents', *J Enzyme Inhib Med Chem* **2014**, *29*, 611-618.
[18] N.-H. Nam, T. L. Huong, D. T. Mai Dung, P. T. Phuong Dung, D. T. Kim Oanh, D. Quyen, L. T. Thao, S. H. Park, K. R. Kim, B. W. Han, J. Yun, J. S. Kang, Y. Kim, S.-B. Han, 'Novel isatin-based hydroxamic acids as histone deacetylase inhibitors and antitumor agents', *Eur. J. Med. Chem.* **2013**, *70*, 477-486.
[19] T. T. L. Huong, D. T. M. Dung, P. T. P. Dung, P. T. Huong, T. K. Vu, H. Hahn, B. W. Han, J. Kim, M. Pyo, S.-B. Han, N.-H. Nam, 'Novel 2-oxoindoline-based hydroxamic acids: synthesis, cytotoxicity, and inhibition of histone deacetylation', *Tetrahedron Lett.* **2015**, *56*, 6425-6429.
[20] T.-T.-L. Huong, D.-T.-M. Dung, N.-V. Huan, L.-V. Cuong, P.-T. Hai, L.-T.-T. Huong, J. Kim, Y.-G. Kim, S.-B. Han, N.-H. Nam, 'Novel N-hydroxybenzamides incorporating 2-oxoindoline with unexpected potent histone deacetylase inhibitory effects and antitumor cytotoxicity', *Bioorganic Chemistry* **2017**, *71*, 160-169.
[21] T. M. D. Do, T. P. D. Phan, T. K. O. Dao, T. H. Pham, T. T. H. Le, D. L. Vu, H. Hyunggu, W. H. Byung, K. Jisung, H. Sang-Bae, N. Nguyen-Hai, 'Novel 3-substituted-2-oxoindoline-based N-hydroxypropenamides as Histone Deacetylase Inhibitors and Antitumor Agents', *Med. Chem.* **2015**, *11*, 725-735.
[22] H. Pham-The, G. Casañola-Martin, K. Diéguez-Santana, N. Nguyen-Hai, N. T. Ngoc, L. Vu-Duc, H. Le-Thi-Thu, 'Quantitative structure–activity relationship analysis and virtual screening studies for identifying HDAC2 inhibitors from known HDAC bioactive chemical libraries', *SAR QSAR Environ. Res.* **2017**, *28*, 199-220.
[23] P.-T. Hai, N. Nguyen-Hai, N. Doan-Viet, H. Dang Thanh, D.-S. Karel, M.-P. Yovani, A. C.-G. Juan, M. C.-M. Gerardo, L.-T.-T. Huong, 'Learning from

Multiple Classifier Systems: Perspectives for Improving Decision Making of QSAR Models in Medicinal Chemistry', *Curr. Top. Med. Chem.* **2017**, *17*, 3269-3288.

[24] D. T. Hieu, D. T. Anh, N. M. Tuan, P.-T. Hai, L.-T.-T. Huong, J. Kim, J. S. Kang, T. K. Vu, P. T. P. Dung, S.-B. Han, N.-H. Nam, N.-D. Hoa, 'Design, synthesis and evaluation of novel N-hydroxybenzamides/N-hydroxypropenamides incorporating quinazolin-4(3H)-ones as histone deacetylase inhibitors and antitumor agents', *Bioorganic Chemistry* **2018**, *76*, 258-267.

[25] P. Skehan, R. Storeng, D. Scudiero, A. Monks, J. McMahon, D. Vistica, J. T. Warren, H. Bokesch, S. Kenney, M. R. Boyd, 'New Colorimetric Cytotoxicity Assay for Anticancer-Drug Screening', *JNCI: Journal of the National Cancer Institute* **1990**, *82*, 1107-1112.

[26] N.-H. Nam, R. L. Pitts, G. Sun, S. Sardari, A. Tiemo, M. Xie, B. Yan, K. Parang, 'Design of tetrapeptide ligands as inhibitors of the Src SH2 domain', *Bioorg. Med. Chem.* **2004**, *12*, 779-787.

[27] B.-S. Min, H.-T.-T. Huong, J.-H. Kim, H.-J. Jun, M.-K. Na, N.-H. Nam, H.-K. Lee, K. H. Bae, S.-S. Kang, 'Furo-1,2-naphthoquinones from Crataegus pinnatifida with ICAM-1 Expression Inhibition Activity', *Planta Med* **2004**, *70*, 1166-1169.

[28] N. H. Nam, D. H. Hong, Y. J. You, Y. Kim, S. C. Bang, H. M. Kim, B. Z. Ahn, 'Synthesis and cytotoxicity of 2,5-dihydroxychalcones and related compounds', *Arch. Pharm. Res.* **2004**, *27*, 581-588.

[29] L. Wu, A. M. Smythe, S. F. Stinson, L. A. Mullendore, A. Monks, D. A. Scudiero, K. D. Paull, A. D. Koutsoukos, L. V. Rubinstein, M. R. Boyd, R. H. Shoemaker, 'Multidrug-resistant Phenotype of Disease-oriented Panels of Human Tumor Cell Lines Used for Anticancer Drug Screening', *Cancer Res* **1992**, *52*, 3029.

[30] Molecular Operating Environment (MOE). 2009.10; Chemical Computing Group ULC, 1010 Sherbooke St. West, Suite #910, Montreal, QC, Canada, H3A 2R7, 2009.

[31] K. Chen, L. Xu, O. Wiest, 'Computational Exploration of Zinc Binding Groups for HDAC Inhibition', *J. Org. Chem.* **2013**, *78*, 5051-5055.

[32] B. E. L. Lauffer, R. Mintzer, R. Fong, S. Mukund, C. Tam, I. Zilberleyb, B. Flicke, A. Ritscher, G. Fedorowicz, R. Vallero, D. F. Ortwine, J. Gunzner, Z. Modrusan, L. Neumann, C. M. Koth, P. J. Lupardus, J. S. Kaminker, C. E. Heise, P. Steiner, 'Histone Deacetylase (HDAC) Inhibitor Kinetic Rate Constants Correlate with Cellular Histone Acetylation but Not Transcription and Cell Viability', *J. Biol. Chem.* **2013**, *288*, 26926-26943.

[33] Y. Hai, D. W. Christianson, 'Histone deacetylase 6 structure and molecular basis of catalysis and inhibition', *Nat. Chem. Biol.* **2016**, *12*, 741-747.

[34] E. Pontiki, D. Hadjipavlou-Litina, 'Histone deacetylase inhibitors (HDACIs). Structure—activity relationships: history and new QSAR perspectives', *Med. Res. Rev.* **2012**, *32*, 1-165.

[35] T. M. D. Do, V. H. Nguyen, M. C. Do, C. H. Dao, H. Pham-The, H. Le-Thi-

Thu, K. Jisung, E. C. Jeong, S. K. Jong, H. Sang-Bae, N. Nguyen-Hai, 'Novel Hydroxamic Acids Incorporating 1-((1H-1,2,3-Triazol-4-yl)methyl)- 3-substituted-2-oxoindolines: Synthesis, Biological Evaluation and SAR Analysis', *Med. Chem.* **2018**, *14*, 831-850.

Exploration of Certain 1,3-Oxazole- and 1,3-Thiazole-Based Hydroxamic Acids as Histone Deacetylase Inhibitors and Antitumor Agents

Duong Tien Anh, Pham-The Hai, Le-Thi-Thu Huong, Eun Jae Park, Hye Won Jun, Jong Soon Kang, Joo-Hee Kwon, Do Thi Mai Dung, Vu Tran Anh, Van Thi My Hue, Sang-Bae Han, Nguyen-Hai Nam

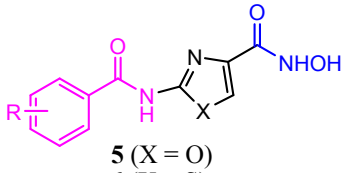

5 (X = O)
6 (X = S)

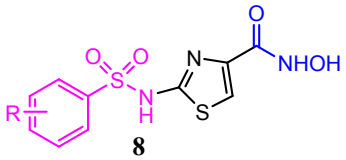

8

Three series of hydroxamic acids (**5a-g**, **6a-g**, **8a-c)** exhibited good cytotoxicity against three human cancer cell lines with IC_{50} values in low micromolar range, comparable to that of SAHA. These compounds also inhibited HDACs with IC_{50} values in sub-micromolar range and some compounds were even more potent than SAHA. Compounds **6a** and **8a** arrested the SW620 cell cycle at G2 phase and significantly induced both early and late apoptosis of SW620 colon cancer cells.

Exploration of Certain 1,3-Oxazole- and 1,3-Thiazole-Based Hydroxamic Acids as Histone Deacetylase Inhibitors and Antitumor Agents

Duong Tien Anh,[a] Pham-The Hai,[a] Le-Thi-Thu Huong,[a] Eun Jae Park, [b]Hye Won Jun,[b] Jong Soon Kang,[c] Joo-Hee Kwon,[c] Do Thi Mai Dung,[a] Vu Tran Anh,[a] Van Thi My Hue,[*,a] Sang-Bae Han,[*,b] Nguyen-Hai Nam,[*,a]

[a]Hanoi University of Pharmacy, 13-15 Le Thanh Tong, Hanoi, Vietnam
[b]College of Pharmacy, Chungbuk National University, 194-31, Osongsaengmyung-1, Heungdeok, Cheongju, Chungbuk, 28160, Republic of Korea
[c]Laboratory Animal Resource Center, Korea Research Institute of Bioscience and Biotechnology, Cheongju, Chungbuk, Republic of Korea

Highlights

- Novel 1,2-oxazole/pyrazole-based hydroxamic acids were synthesized.
- The 1,2-oxazole/pyrazole-based hydroxamic acids exhibited potent HDAC inhibition.
- The 1,2-oxazole/pyrazole-based hydroxamic acids exhibited good cytotoxicity.
- Compounds **6a** and **8a** induced apoptosis and arrested SW620 cell cycle at G2 phase.

Exploration of Certain 1,3-Oxazole- and 1,3-Thiazole-Based Hydroxamic Acids as Histone Deacetylase Inhibitors and Antitumor Agents

Duong Tien Anh,[a] Pham-The Hai,[a] Le-Thi-Thu Huong,[a] Eun Jae Park, [b]Hye Won Jun,[b] Jong Soon Kang,[c] Joo-Hee Kwon,[c] Do Thi Mai Dung,[a] Vu Tran Anh,[a] Van Thi My Hue,[*,a] Sang-Bae Han,[*,b] Nguyen-Hai Nam,[*,a]

[a]*Hanoi University of Pharmacy, 13-15 Le Thanh Tong, Hanoi, Vietnam*
[b]*College of Pharmacy, Chungbuk National University, 194-31, Osongsaengmyung-1, Heungdeok, Cheongju, Chungbuk, 28160, Republic of Korea*
[c]*Laboratory Animal Resource Center, Korea Research Institute of Bioscience and Biotechnology, Cheongju, Chungbuk, Republic of Korea*

The authors declare no conflict of interests.